CHEMPHYSCHEM
Reviews

Methods for Improving the Lifetime Performance of Organic Photovoltaics with Low-Costing Encapsulation

Myrsini Giannouli,*[a, b] Vasileios M. Drakonakis,[b] Achilleas Savva,[b] Polyvios Eleftheriou,[b] Georgios Florides,[b] and Stelios A. Choulis[b]

These are not the final page numbers! ↗↗
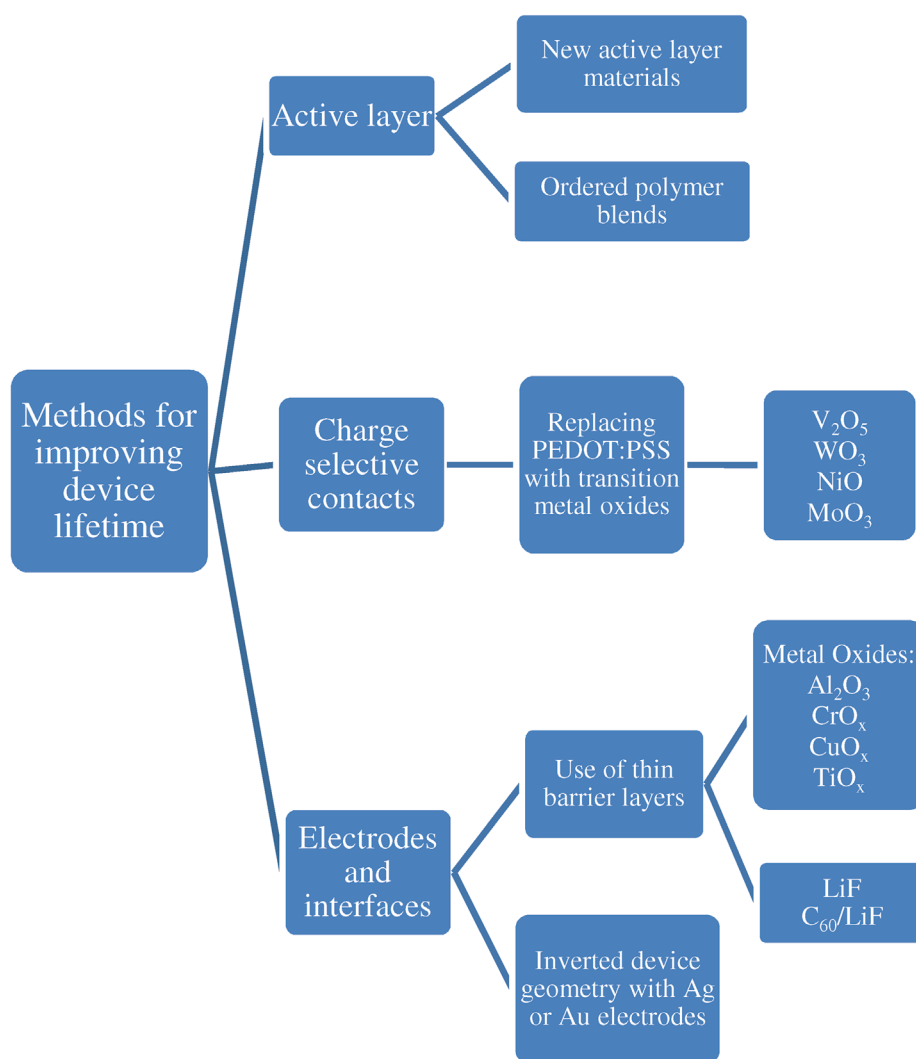
Recent years have seen considerable advances in organic photovoltaics (OPVs), most notably a significant increase in their efficiency, from around 4% to over 10%. The stability of these devices, however, continues to remain an issue that needs to be resolved to enable their commercialization. This review discusses the main degradation processes of OPVs and recent methods that help to increase device stability and lifetime. One of the most effective steps that can be taken to increase the lifetime of OPVs is their encapsulation, which protects them from atmospheric degradation. Efficient encapsulation is essential for long-term device performance, but it is equally important for the commercialization of OPVs to strike a balance between achieving the maximum device protection possible and using low-cost processing for their encapsulation. Various encapsulation techniques are discussed herein, with emphasis on their cost effectiveness and their overall suitability for commercial applications.

1. Introduction

1.1. Organic Photovoltaics: Advantages and Recent Breakthroughs

Photovoltaic technology is considered one of the most promising alternatives to fossil fuels, as it provides a source of energy that is both sustainable and environmentally friendly.[1] The photovoltaic market has experienced a rapid growth over the past two decades,[2] and so far it has been largely dominated, to over 90%, by silicon-based solar cells.[3] Si-based photovoltaics have been researched extensively, and they yield efficiencies of around 30% in single-junction cells.[4] Figure 1 demonstrates the highest research efficiencies for various solar-cell technologies.

From a purely economic standpoint, however, silicon solar cells are still far from being competitive with conventional energy sources. Organic photovoltaics (OPVs) represent a low-
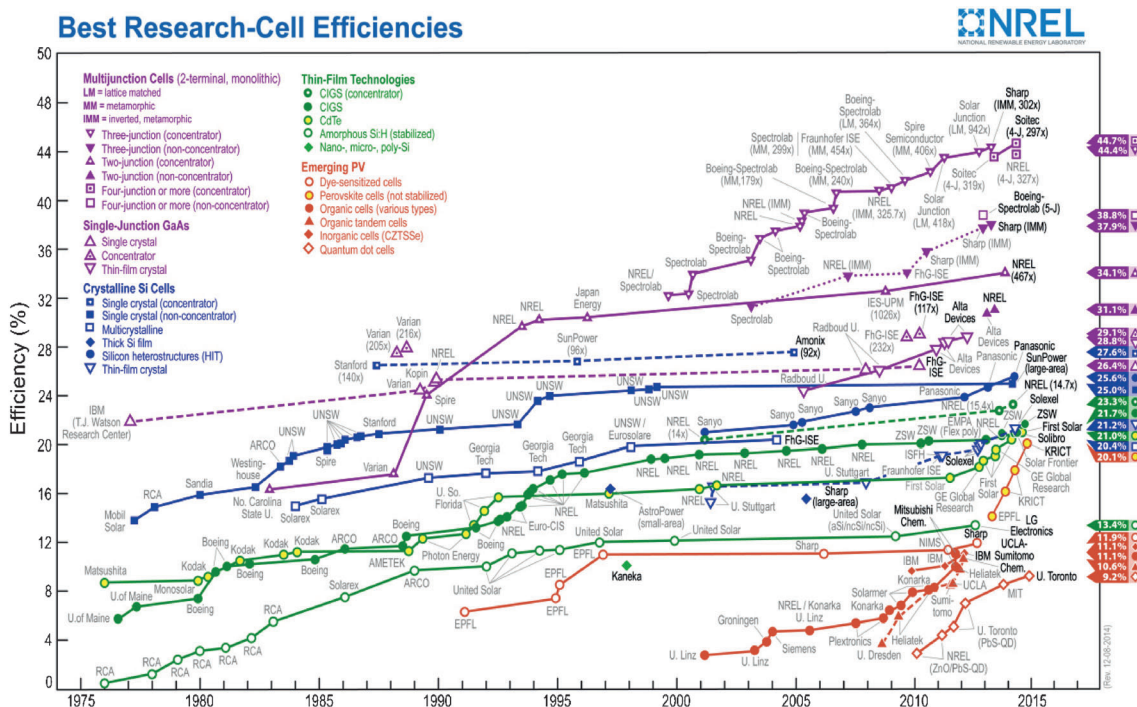
Figure 1. Best research solar-cell efficiencies. Compiled from ref. [18].

[a] Dr. M. Giannouli
Renewable Energy and Environment Laboratory,
Physics Department, University of Patras,
26500 Patras (Greece)
E-mail: myrgiannouli@upatras.gr

[b] Dr. M. Giannouli, Dr. V. M. Drakonakis, A. Savva, Dr. P. Eleftheriou,
Dr. G. Florides, Prof. S. A. Choulis
Molecular Electronics and Photonics Research Unit,
Department of Mechanical Engineering and Materials Science and Engineering,
Cyprus University of Technology,
Limassol, 3041 (Cyprus)

Special Issue — An invited contribution to a Special Issue on Organic Electronics

cost alternative, due to the high optical absorption coefficients of organic semiconductors, which enable the development of efficient photovoltaic devices with layers only a few nanometers thick. In addition to their low cost, OPVs have other advantages over conventional Si-based photovoltaics, such as environmentally friendly degradability, flexibility, and low weight, which unlock new applications for the use of photovoltaic electricity.[5] Furthermore, their solubility in common organic solvents makes them processable with various roll-to-roll[6] and printing[7] techniques.

Dr. Myrsini Giannouli received her B.S. and M.S. degrees in Physics from the University of Manchester, UK, and she was awarded a Ph.D. degree in Mechanical Engineering from the Aristotle University of Thessaloniki, Greece, in 2006. She has since worked as a postdoctoral research associate and lecturer at the University of Patras, Greece, and at the Cyprus University of Technology. Myrsini currently holds a postdoctoral research position in the Department of Physics, University of Patras. Her research activities include the study of energy production and conservation systems, with an emphasis on the development and optimization of photovoltaic devices.

Dr. Vasileios (Vassilis) Drakonakis received his Diploma in Mechanical and Aeronautics Engineering from the University of Patras, Greece, in 2008 and his Ph.D. degree in Industrial Manufacturing and Systems Engineering from the University of Texas at Arlington in 2012. He has a transdisciplinary background in industrial, mechanical, and chemical engineering. In 2012, he joined the Molecular Electronics and Photonics Research Unit at the Cyprus University of Technology as a postdoctoral fellow under Professor Choulis. His expertise is in applied mechanics and materials processing and characterization. His current research interests focus on the lifetimes of organic electronics, packaging, and flexible substrates as well as scaled-up manufacturing.

Achilleas Savva received his B.S. and M.S. degrees in Chemical Engineering from Aristotle University of Thessaloniki in 2010. Since 2011, he has been a member of the Molecular Electronics and Photonics Research Unit at Cyprus University of Technology (CUT) and a Ph.D. candidate/research associate in the Department of Mechanical Engineering and Materials Science and Engineering at CUT, under the supervision of Professor Choulis. His current research interests lie in the area of understanding the interfaces of solution-processed inverted organic solar cells.

Dr. Polyvios Eleftheriou received his B.S. degree in Mechanical Engineering from Tennessee Tech University in the USA in 1982 and his M.S. and Ph.D. degrees from the same university in 1984 and 1987, respectively, under the supervision of Professor W. B. Swim. After a year of postdoctoral research in the laboratory of Professor Swim (Center of Excellence for Manufacturing Research), he accepted a position at the Higher Technical Institute in Nicosia as a lecturer in 1988. In 2008, he joined the Cyprus University of Technology. His research interests include energy-related subjects.

Dr. Georgios Florides received his basic degree in Mechanical Engineering from the Higher Technical Institute of Cyprus, and he was awarded M.Phil. and Ph.D. degrees by Brunel University, London, UK. After long-term employment in the Engineering Practice Department of the Higher Technical Institute he accepted the position of Senior Lecturer in the Department of Mechanical Engineering of the Cyprus University of Technology. His research activities focus on the topic of energy and renewable energy. He is also a recognized supervisor of Brunel University, UK.

Professor Stelios A. Choulis is the Departmental Chair of Mechanical Engineering and Material Science and Engineering at the Cyprus University of Technology (CUT) and the head of the Molecular Electronics and Photonics Research Unit at CUT. He served as the device research and development (R&D) group leader of Konarka Technologies (2006–2008), R&D member of Osram Opto-Semiconductors, Inc., and light-emitting diode R&D team at Silicon valley (2004–2006). During pursuit of his Ph.D. degree (University of Surrey, UK) and his first postdoctoral research fellowship position at the Advanced Technology Institute (1999–2002, University of Surrey, UK), both funded by the EPSRC, he investigated the optical properties of quantum electronic materials and optoelectronic devices. In 2002, he joined the Center of Electronic Materials and Devices (Imperial College London, UK) as a postdoctoral research associate, funded by British Petrol, and work on the optoelectronic properties of molecular semiconductor materials and devices (2002–2004). Dr. Choulis' research interests focus on solution-processed optoelectronic materials and devices for cost-effective printed and flexible electronics applications.

The aforementioned advantages of OPV devices have led to increased interest in their development and, as a result, to considerable progress towards improving their performance.[8] The power conversion efficiency (PCE) of OPVs has increased from 6% in 2009[9, 10] to 7.4% in 2010[11] and to 8.3% in 2011.[12] In 2012, this number rose to 9.1%,[13] only for this record to be broken shortly thereafter by the German company Heliatek, who announced the production of a 1.1 cm^2 tandem organic cell with an impressive PCE of 10.7%.[14] The same year, the Mitsubishi Chemical Corporation announced that the conversion efficiency of its organic thin-film photovoltaic (PV) cell had reached 11.0%.[15] Heliatek broke its own record in January 2013 by announcing 12.0% efficiency, again for a 1.1 cm^2 organic cell by using two patented absorber materials.[16] Laboratory efficiency of 8.0% was also recorded the same year for a single-junction cell by using a 2D conjugated small molecule as a donor, and 10.1% efficiency was recorded for tandem cells by using the same small molecule.[17]

The highest efficiencies documented in recent years[18] are shown in Table 1, which also summarizes the main characteristics of the devices used to achieve these record efficiencies.

Table 1. Overview of OPV performance milestones in recent years and main device characteristics.

Efficiency [%]	Year	Active layer	Structure
6.1[9]	2009	PTB4/PC$_{61}$BM	normal
6.1[10]	2009	PCDTBT/PC$_{70}$BM	normal
7.4[11]	2010	PTB7/PC$_{71}$BM[a]	normal
8.3[12]	2011	Power Plastic (Konarka)	normal
9.1[13]	2012	ActivInk PV2000 (Polyera)	inverted
10.7[14]	2012	Oligomers Smolecules (Heliatek)	tandem
12.0[16]	2013	two patented (Heliatek) materials with different absorption wavelengths	tandem

[a] PTB7 = poly({4,8-bis[(2-ethylhexyl)oxy]benzo[1,2-b:4,5-b']dithiophene-2,6-diyl}{3-fluoro-2-[(2-ethylhexyl)carbonyl]thieno[3,4-b]thiophenediyl}).

Current scientific interest in OPV technology is not only directed towards increasing their PCE. In recent years, there has been increased interest in understanding the degradation mechanisms of OPVs, and considerable efforts have been focused towards increasing their lifetime. Recent breakthroughs in the field have succeeded in increasing the lifetime of OPVs from mere minutes to many thousands of hours.[19] Several new developments have contributed towards the direction of increased OPV stability, such as inverted device structures[13] (which allow for highly stable metal electrodes), utilization of highly photostable active materials,[20] introduction of interfacial layers,[21] and the use of advanced packaging techniques.[22]

In this review, we discuss recent scientific progress in improving the stability and lifetime of OPVs, with an emphasis on devices sealed primarily with low-costing materials.

A short overview of the main degradation mechanisms that take place in common types of OPV devices is presented in Section 2 of this review. Recent progress and current state-of-the-art on improving device stability are discussed in Section 3,

whereas the effectiveness (including cost considerations) of various materials (including low-costing ones) and methods for encapsulating OPV devices are assessed in Section 4.

1.2. Commercialization of OPVs

The successful commercialization of OPV technology cannot be based solely on achieving high PCEs. The technology also has to become cost competitive with conventional power generation.[23] The cost-effective deployment of photovoltaic (PV) systems is based on the following key requirements[24] (Figure 2):

1) Minimum system cost.
2) Maximum initial performance.
3) Minimum loss of performance over time.
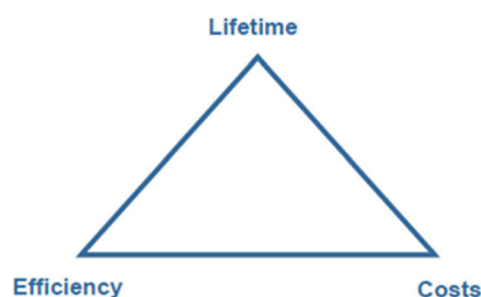
Figure 2. The critical triangle for photovoltaics. Organic solar cells have to simultaneously fulfill all requirements: lifetime, efficiency, and cost. Reprinted with permission from ref. [29]

One of the aspects of OPVs that hinders their commercialization is their low stability and overall lifetime.[25] The conjugated organic materials that comprise all OPV devices (bulk heterojunction) are more susceptible to photodegradation and degradation from oxygen and water than inorganic materials. Crystalline Si-based solar cells have lifetimes of over 25 years, and although lifetimes of several thousands of hours have been reported for OPVs, the latter must be significantly improved for OPV technology to become competitive with conventional solar-cell technologies.[26] Nevertheless, as previously mentioned, neither the lifetime nor the efficiency of an OPV device should be considered individually upon competing with other solar-cell technologies. All three of the parameters highlighted in Figure 2 need to be simultaneously taken into account, and it is in the third parameter, the cost, that one of the main advantages of this emerging technology lies.

The low-cost manufacturing processing that is used to produce OPVs is a strong advantage, and it is expected to make this technology competitive with conventional energy sources in certain markets. Such devices would be especially suitable for off-grid applications, for example, in third-world or developing countries.[27,28] Given that polymers are usually processed in the liquid phase, simple printing and coating techniques can be utilized.[29,30] It has been observed that the overall cost of screen-printed OPVs depends largely on the cost of the ink

↖↖ **These are not the final page numbers!**

used, as well as on the labor cost used for their production.[31] Manufacturing OPVs fully by roll-to-roll processes can reduce production costs considerably by minimizing manual labor costs. OPV modules with lengths up to 25 cm have been successfully produced by using roll-to-roll processes, such devices can be manufactured with electricity costs as low as 8.1 € per Watt-peak ($€W_p^{-1}$).[28,32,33] In the future, upon optimization of large-scale production processing, organic solar cells can become even more cost effective.[29] It is estimated that, as the technology matures, manufacturing costs will decline, whereas the efficiency and lifetime of the devices will increase.[34] Recently, Machui et al.[35] demonstrated that a cost of 1–$8.4 €W_p^{-1}$ could be achieved for single-cell and tandem modules with two different active-layer donor materials (low- and high-cost scenarios). The highest contributors to the overall device cost have been identified to be the active-layer materials, the electrodes, and the barrier foils. Future production forecasts for an industrial processing scenario indicate that OPVs can be manufactured at an even lower cost, in the range of 0.05 to $0.6 €W_p^{-1}$, depending on device efficiency, material choice, and structure.[35]

Another important characteristic of OPVs is that printing and coating manufacturing techniques can be entirely conducted on flexible substrates;[36] this enables the production of flexible devices that are suitable for a wider range of applications than conventional nonflexible solar cells.[7]

1.3. Developing Cost-Effective OPVs

A recent study[37] estimates that the manufacturing cost of purely organic solar cells ranges between 50 and $140\ \$m^{-2}$ (low- and high-cost scenarios), depending on the materials and processes used. These manufacturing costs lead to electricity costs ranging between 49 and $85 ¢kWh^{-1}$. To achieve a more competitive electricity cost of about $7 ¢kWh^{-1}$ with the same production costs, the efficiency of OPVs would have to increase to 15% and their lifetime would have to increase to between 15 and 20 years.[37] Given that OPV technology is not yet mature enough to attain these efficiency and lifetime goals, it becomes very important to limit the production costs of the cells as much as possible, without compromising their performance. According to the low-cost scenario ($50\ \$m^{-2}$),[37] approximately half of the overall production costs originate from the materials required for OPV production. Table 2 presents the cost estimates for OPV materials for both low- and high-cost scenarios.

On the basis of Zweibel's work,[38] approximately 10% of overall production costs typically originate from the packaging material. In the aforementioned low-cost scenario (overall cost

Table 2. Materials cost estimates for OPVs. Reprinted with permission from ref. [37].

Cost component	Organic solar cell Type used[a]	Cost estimate [$ m^{-2}$]	
		Low	High
semiconductor	C_{60}, CuPc&SnPc	3.30	5.00
electrical contacts and interconnects	aluminum, silver paint	3.40	5.00
substrate[b]	flexible plastic, ITO	7.90	13.68
protective cover	flexible encapsulant	2.90	4.40
sealant	Surlyn	2.90	4.40
packaging material	–	2.00	3.00
specialty chemicals	4TBP	1.00	2.00
other (absorbing dye, catalyst, electrolyte)	N/A[c]	N/A[c]	N/A[c]
total		23.40	37.48

[a] CuPc&SnPc = copper(II) phthalocyanine & tin (II) phthalocyanine, 4TBP = 4-tertiary butyl phenol. [b] There are two substrates, hence the estimates are for the two substrates, not just one. [c] N/A = not available.

$50\ \$m^{-2}$),[37] cheap packaging materials were considered ($2.00\ \$m^{-2}$ as estimated by Zweibel). Thus, the cost of the packaging material for the low-cost scenario would amount to less than 5% of the overall production cost. The use of higher costing packaging materials, however, could increase the packaging cost and would also increase the overall cost of the cell. To keep OPV production costs as low as possible, it is important to use packaging materials that are as low costing as possible.

On the other hand, packaging of the devices is conducted to protect them from degradation in the presence of oxygen and moisture. For that reason, packaging is directly related to the lifetime of the devices. As such, the use of low-costing packaging materials that keep the production cost down is essential, however, only if they simultaneously provide effective sealing of the device, which thus impedes its degradation.

2. Main Degradation Mechanisms

2.1. Overview

In general, organic solar cells degrade because of their low resistance to water, oxygen,[39] high temperatures,[40,41] light exposure, and so on. The conjugated polymers that comprise the active blend of OPVs have long been known to be unstable in air[42] and to react by photolytic and photochemical reactions if exposed to sunlight, some of which cause photodegradation of the polymer.[43] The photodegradation of the conducting polymers is a very serious disadvantage to their use in OPV devices, as solar cells are subjected to extensive illumination. Moreover, not only light, but also the presence of atmospheric components such as water and oxygen can cause reactions with certain polymers used in OPVs that eventually lead to their rapid deterioration.

In addition to the degradation of the active layer, another major cause of rapid OPV degradation is the susceptibility of low work function metals (used for the nontransparent electrode) to oxidation in the presence of absorbed oxygen molecules.[44] The degradation of the metal electrode leads to the formation of thin insulating oxide barriers between the metal

These are not the final page numbers! ↗↗

and the polymer layers, which hinders electric conduction and collection of the charge carriers.[45] The interfaces between the various layers are also subject to degradation, as, for example, the degradation of the interface between the metallic contact and the organic semiconductors through an electrochemical process.[46]

The above are only some of the degradation mechanisms that take place in OPVs, so it is easy to understand that the development of such devices with high stability is not an easy feat. As the materials that constitute the device deteriorate, so do their physical, electrical, and mechanical properties.[47] All the processes that are necessary for the operation of OPVs, such as charge-transfer processes, are delicate and sensitively affected by any reactions that may occur both within the bulk of the polymer blend and the interfaces. Deterioration of any part of the device will eventually lead to a reduction in device performance.[48] Thus, comprehending the nature of the degradation mechanisms in OPVs will greatly contribute towards the development of highly stable devices.

Figure 3 depicts some of the numerous reactions and processes that are responsible for the rapid aging of organic solar cells.[49]

The processes in this figure include (shown from left to right) water-induced degradation of the transparent electrode [i.e. indium tin oxide (ITO)]; the photodegradation of the polymers and also their degradation by oxygen or water, which leads to the formation of polymer/oxide composites; and finally the susceptibility of the metal electrode to reactions with oxygen and water.

Various methods have been employed to assess the stability and lifetime of OPVs. Concentrated light has been used successfully to perform accelerated photochemical degradation of polymer solar-cell materials.[50] It has been established that at high solar intensity concentration (over 100 sun), the same degradation behavior is observed as for 1 sun, only on a shorter timescale.[51] This method can thus provide a highly accelerat-

ed evaluation of polymer degradation and stability. Recently, a global consortium was developed to evaluate the lifetime and stability of OPVs. Most researchers currently follow the recommendations that have been established by the consortia of the international summit on OPV stability (ISOS) as a reference to accurately determine the stability of devices under certain predefined environmental lifetime conditions. The application of lifetime conditions is described within the ISOS protocols.[52,53]
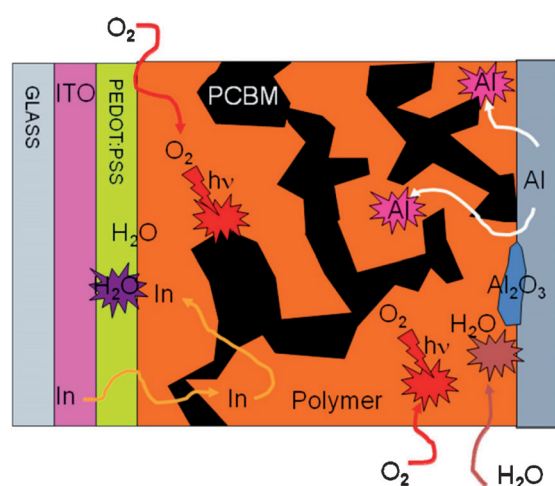
The degradation mechanisms of OPVs have been investigated in many recent studies by subjecting the devices to accelerated illumination conditions[52] under the aforementioned ISOS protocols.[53,21] Later, these particular OPV devices (both normal and inverted OPVs)[20] were characterized through time-of-flight secondary ion mass spectrometry (TOF-SIMS),[54] incident photon-to-electron conversion efficiency (IPCE),[55] and imaging techniques (techniques such as laser beam induced current, electroluminescence imaging, photoluminescence imaging, dark-lock in thermography).[56] A number of different degradation mechanisms have been observed through these advanced characterization techniques, including[54–56] oxidation of metal electrodes (such as Al), blocking contact formation, electromigration of Ag (inverted OPVs), water and oxygen ingress, water release from the highly conductive part of poly(3,4-ethylenedioxythiophene):polystyrene sulfonate) (PEDOT:PSS), and dissolution of either the metal or PEDOT:PSS within the active layer {poly(3-hexylthiophene):[6,6]-phenyl-C_{61}-butyric acid methyl ester (P3HT:PCBM)}. These degradation mechanisms are described in the following sections.

2.2. Degradation of Polymer Donors Commonly Used in OPVs

The degradation of the conjugated polymers, which constitute the active layer of OPVs, plays an important role in the reduced lifetime of the devices.[26,57] Photodegradation reactions that take place upon illumination of OPVs, especially in the presence of oxygen, lead to degradation of the active layer.[58] These reactions cause chemical changes in the active layer, which results in low device stability. Most conjugated macromolecules have low photochemical stability, which leads to reduced device lifetime. Exposure of such polymers to UV/Vis light leads to the destruction of the π-conjugated system, which results in a decrease in the absorbance of the polymer blend.[58]

The first polymer solar-cell devices were based on poly(para-phenylenevinylene) (PPV) materials. Over the years, there has been considerable progress towards understanding the degradation mechanisms of PPV-based devices, and their stability and lifetime have been thoroughly investigated.[59–61] It has been reported that PPV and its derivatives are especially vulnerable to atmospheric degradation,[62] and this process occurs through the binding of oxygen atoms to vinyl bonds, which breaks the conjugation and leads to the formation of carbonyl groups.[63,64]

Another conjugated polymer family that has been used extensively in OPVs is the polythiophenes and especially P3HT.

Figure 3. Cross-section view of a solar cell with the several processes that conspire to degrade polymer solar cells. A schematic illustration of some of the degradation mechanisms that take place in a typical bulk heterojunction are shown. Reprinted with permission from ref. [49].

⬉⬉ These are not the final page numbers!

The stability and lifetime of P3HT devices have been investigated extensively,[65] and studies comparing the stability of PPV and polythiophene-based OPVs have shown that the polythiophenes are considerably more stable under illumination than PPV derivatives.[66] However, P3HT films suffer from degradation under illumination as well. The effects of illumination on P3HT films have been investigated, and illumination of the films causes an increase in trap density and a decrease in hole mobility.[67]

Understanding the degradation processes of polythiophenes will enable the development of new polymers with enhanced stability. However, the mechanism responsible for the degradation of P3HT has been the subject of some debate. It was originally thought that the chemical reaction responsible for its degradation was a direct attack by singlet oxygen on the thiophene ring.[68] This is still the prevalent theory for the degradation of P3HT in solution. However, the thermo- and photodegradation mechanisms of bulk P3HT have been recently reconsidered,[69] through exposure of P3HT films to UV/Vis-light irradiation and thermal ageing, and a degradation mechanism that accounted for the modifications in the infrared spectra of aged films has been developed (see Figure 4). It was observed that under both ageing conditions the alkyl groups and thiophene rings of P3HT disappeared, and it was shown that singlet oxygen plays a lesser role than previously reported. Instead, oxidation was shown to involve the radical oxidation of the n-hexyl side chains with subsequent degradation of the thiophene rings. The breaking of the macromolecular backbone resulted in a loss of π-conjugation and a decrease in the UV/Vis absorbance; this led to eventual degradation of the polymer. In addition, it has been reported[70] that the presence of humidity strongly affects this degradation process, although water itself does not decompose the polymer. The influence of the microstructure of P3HT on its photodegradation has also been studied,[71] and high-regioregular P3HTs are more photostable than low-regioregular P3HTs because of their higher crystallinity and purity.

2.3. Degradation of the Active Layer

2.3.1. Light-Induced Degradation

The long-term stability of the active layer under illumination is one of the most important parameters that has to be taken into account to achieve high OPV performance and lifetime. Especially, the behavior of the active layer under illumination in the absence of oxygen is a subject of considerable scientific interest, as it is universally accepted that effective OPV devices will require some type of encapsulation to protect them from degradation.[72] It has been observed[64] that the photochemical stability of P3HT:PCBM blends on inert substrates is high in the absence of oxygen. In the absence of oxygen, degradation is attributed first to the photochemical instability of P3HT[66] and second to the blend's morphological instability.[73] It has also been observed that the chemical stability of the active layer depends on the polymer/fullerene ratio in the active-layer blend. PCBM can act as a stabilizer to the more unstable PPV derivatives,[74] so a higher concentration of PCBM in the blend can result in more stable OPV devices, and this has been attributed to the formation of large PCBM areas.[75] More recently, however, it was shown that although PCBM stabilizes other polymers, such as P3HT films, upon exposure to air, its fullerene cage undergoes a series of oxidations that contribute to the deterioration of the photoconductivity of the blend.[76]

The effect of light on the morphology of the polymer blend has been established through optical microscopy studies.[64] It has been shown that after 3000 h of continuous illumination in the absence of oxygen, textural changes start to appear in the active layer due to photodegradation (Figure 5a). The effect of these reactions on the active layer, however, is not as significant as that of photodegradation reactions in the presence of oxygen.[77]

The degradation of the active layer under illumination in the presence of oxygen is a complex process that has not been thoroughly investigated to date. The decay mechanisms of non-encapsulated P3HT:PCBM devices under illumination in the presence of oxygen have been studied.[78] Two primary loss
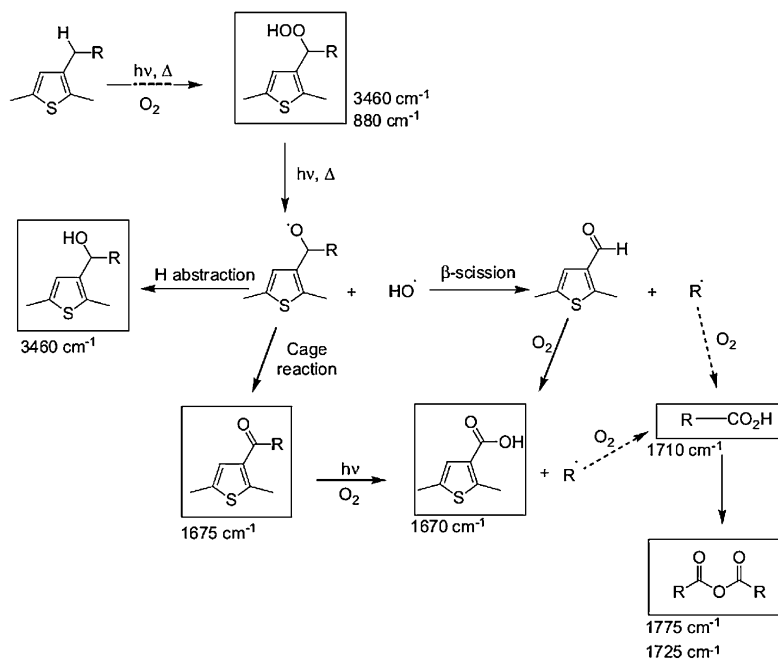
Figure 4. a) Oxidation mechanism of the P3HT alkyl side chain. b) Oxidation mechanism of the sulfur atom of the thiophene ring. Reprinted with permission from ref. [69].
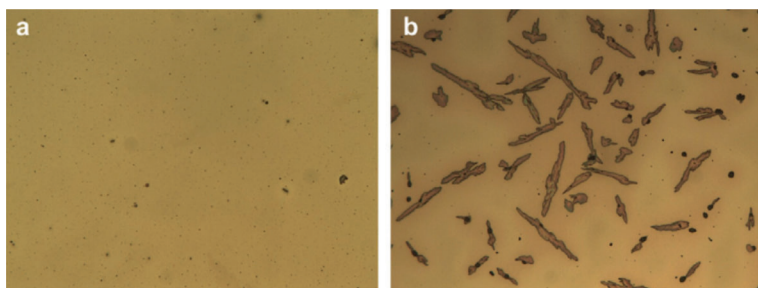
Figure 5. Optical microscopy images of P3HT:PCBM films a) after 3000 h exposure in the absence of oxygen to yield the formation of small spots and b) after 100 h thermal annealing at 100 °C (in the absence of light) to yield the formation of large PCBM clusters (images size: 1000 mm). Reprinted with permission from ref. [64].

mechanisms for the efficiency of these devices have been identified. The first consists of an initial ultrafast decrease in polaron generation, and the second consists of a loss in the exciton population within the photoexcited P3HT domains. It has been observed that the oxidation of PCBM results in the formation of species with up to eight oxygen atoms, which act as electron traps.[76] It has also been reported that the formation of such electron traps under oxidation decreases carrier mobility in OPVs and results in significant loss of current.[79]

2.3.2. Thermal Degradation

Most polymer blends used in OPVs are not thermodynamically stable, but nonequilibrium states lead to macrophase separation of the blend during extended operation and ultimately to decreased device performance.[80] Additional instability can occur from the diffusion of PCBM during device preparation and use. This effect gives rise to concentration gradients, depletion from active areas of the device, and, in some cases, aggregation or crystallization of PCBM.[81] It has also been observed that the interface between the cathode and the active layer in OPV devices is thermally unstable.[82]

The effect of heat on the active layer has been reported to be considerable, and it has been shown that prolonged (100 h) annealing at 100 °C can lead to phase separation and PCBM crystallization.[64] In this case, PCBM vanishes from the P3HT:PCBM matrix, segregates, and gathers in clusters observed as black large zones (Figure 5 b). Such extreme morphological changes do not appear in the active layer after illumination, which confirms that it has a relatively high degree of photolytic stability. It has also been reported that that active-layer annealing at 130 °C for only 5 h leads to degradation of the alkyl groups and thiophene rings in the polymer blend, a decrease in the UV absorbance, and, ultimately, a significant drop in the power conversion efficiency of the OPVs.[83]

More recently, the role of the annealing processing step within the device fabrication has been investigated. It has been found that annealing also influences the cohesion/adhesion properties of the active layer, an important parameter for lifetime performance.[84]

Finally, Sachs-Quintana et al.[85] have recently demonstrated the superiority of the inverted structure over the normal structure under exposure to heat; this underlines the importance of the architecture on the charge flow and interfacial properties. It is suggested that the first step in thermal degradation is due to electron-barrier formation, an effect that is more intense in normal OPV device architectures.[85]

2.3.3. Degradation by Oxygen and Water Molecules

As mentioned above, organic materials are sensitive to water and oxygen, so penetration of these molecules into the device can lead to deterioration of the active layer.[86] The active layer is usually well protected against atmospheric agents, not only by encapsulation, but also from other layers in the device that act as barriers.[87] However, some water and oxygen molecules can slowly diffuse through the various layers of the device to reach the active layer and to react with the polymer materials, which causes their degradation.[88] The effect of water on the performance of OPV devices has been studied, and it has been observed that the presence of moisture within bulk polymers initiates a stronger recombination process that decreases the ability of charge generation in the bulk-heterojunction area.[84]

Isotopic labeling and mass spectrometry imaging have been used successfully to map out oxygen and water processes through the various layers of the OPV devices. Oxygen[89] and water[47] molecules may diffuse into the device through the metal electrode and permeate through all the layers of the device all the way to the counter (transparent) electrode. Oxygen and water molecules gain entry to the device through microscopic pinholes in the metal electrode.[19] Evidence of the diffusion of water into the device through the aluminum electrode has also been presented for a number of different polymer blends.[90,91] It has also been reported that oxygen molecules are especially more harmful to P3HT:PCBM cells under illumination than in the dark.[92]

2.4. Degradation of the Hole-Transport Layer

In most OPV devices, PEDOT:PSS is used for the transfer of holes between the transparent electrode and the active layer for normal structures and between the metal electrode and the active layer for inverted structures. Even though the hole-transport layer is essential to the efficient function of OPV devices, the degradation of PEDOT:PSS can shorten the lifetime of the devices. Moreover, the properties of this layer can cause increased degradation in other layers as well.

PEDOT:PSS is especially vulnerable to thermal degradation. Even though it has been shown that heat treatment of PEDOT:PSS films for up to 10–20 min can be beneficial for the electrical properties of the films,[93] prolonged exposure to high temperatures may cause their thermal degradation. Studies of the thermal stability of this material have shown that its exposure to a temperature of 120 °C for over 55 min can significant-

↖↖ **These are not the final page numbers!**

ly reduce its electrical conductivity.[94] In this case, aging is due to shrinking of the PEDOT conductive grains. However, annealing of PEDOT:PSS films at lower temperatures can help increase their electrical conductivity due to thermal activation of the carriers and an improvement in crystallinity.

The PEDOT:PSS layer is also very sensitive to moisture and oxygen. The detrimental effects of atmospheric air on the electrical properties of this material have been studied.[95] The PEDOT:PSS layer is highly hygroscopic, and if it absorbs water, its conductivity decreases and consequently the device lifetime shortens. Figure 6 shows the change in conductivity of PEDOT:PSS films with respect to heating time, under an inert atmosphere and in air. From this figure it can be observed that the presence of oxygen and moisture promotes irreversible structural modifications of the PEDOT:PSS chains, and this reduces its conductivity.
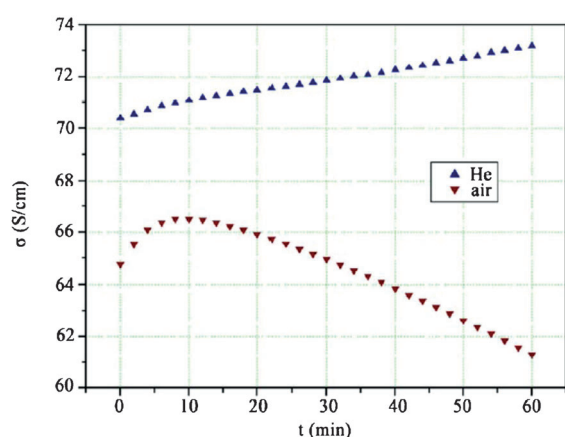
Figure 6. Change in the conductivity of two PEDOT:PSS 120 nm thick films, as a function of heating time (t) at 443 K under an inert atmosphere of He and in atmospheric air. Reprinted with permission from ref. [95].

The PEDOT:PSS layer can also increase the degradation of other layers of OPV devices. It has also been observed that water absorbed by the PEDOT:PSS layer can diffuse through the device all the way to the metal cathode,[96] which accelerates degradation of the metal electrode and thus reduces device lifetime.

Moreover, the PEDOT:PSS layer can increase the degradation of the active layer. Studies on poly[2-methoxy-5-(3′,7′-dimethyloctyloxy)-1,4-phenylenevinylene] (MDMO-PPV)/PCBM OPVs have shown that the degradation is associated with water absorption into the PEDOT:PSS layer, and charge-transport measurements revealed that the effect of water on PEDOT:PSS is to increase the sheet resistance of the PEDOT:PSS/blend layer interface.[39] It has also been reported that the PEDOT:PSS layer can induce degradation of the active layer in P3HT:PCBM OPVs, which is demonstrated by a decrease in the absorbance and the formation of aggregates in the active layer.[58]

Recently, it was demonstrated that the addition of processing additives to PEDOT:PSS significantly enhances hole-carrier selectivity in inverted solar cells.[97] Comparison between normal and inverted OPVs under ambient illumination has shown that the former degrade much more quickly due to oxidation of the top metal (such as Al).[98] In the case of inverted OPVs, Krebs et al. have shown that the main degradation mechanism for inverted OPVs in a dark ambient environment is due to phase separation of PEDOT:PSS (water and oxygen molecule absorbance) as well as to the interaction at the active layer/PEDOT:PSS interface.[92] By using reverse engineering methods it was recently shown that the PEDOT:PSS hole-selective contact is the major degradation mechanism for inverted OPVs under accelerated lifetime humidity conditions.[91]

2.5. Degradation of the Metal Electrode

Certain metals such as Al, Ca, and Ag are commonly used as electrodes in OPV devices because of their high electrical conductivity, work function properties, and ability for deposition as very thin layers. Degradation of the metal electrode contributes to the overall reduction in cell performance, and its origin has been the subject of several recent studies.[99]

Two main degradation mechanisms of the metal electrode have been identified: one, its oxidation at the metal/polymer interface and/or at the upper surface of the metal layer;[100] two, its chemical interaction with polymers at its interface with the active layer.[101]

The first mechanism, the degradation at the electrode/polymer interface, can result in the formation of an oxidation layer at the metal/polymer interface.[102] This oxidation layer hinders charge selectivity of the electrode, which thus reduces device performance. For Ca/Al electrodes, it has been reported that their degradation in air is due to considerable changes at the metal–organic interface.[100] Cross-sectional TEM studies have revealed the formation of void structures to be the primary degradation mechanism for Ca/Al contacts. These structures grow as the electrode ages and becomes oxidized, as shown in Figure 7.[101] For Ag contacts, it has similarly been observed that the electrode becomes oxidized and that an interfacial layer of silver oxide is formed over time, but its formation is a much longer process than for Al-based electrodes.[99]

The second degradation mechanism of the metal electrode, its chemical reaction with the active layer, has also been investigated,[92] and this mechanism involves the chemical interaction of the thiophenes in P3HT with the top metal electrodes.[101] For example, Cu electrodes have been found to react with sulfur sites on P3HT during the deposition process.[103] It has also been observed that aluminum penetrates into the active layer, which results in the gradual formation of Al–C bonds. A diffused organic–Al interface is formed, which then results in a large oxidized interfacial area upon air exposure. It has been shown that Al interacts with C_{60} to form Al–C_{60} bonds that cause reduced charge transport and device performance.[104, 105]

2.6. Degradation of the Transparent Electrode

By the term "transparent electrode" we refer to the electrode that constitutes either the anode in normally structured OPVs [which usually consists of a transparent conductive oxide

These are not the final page numbers! ↗↗
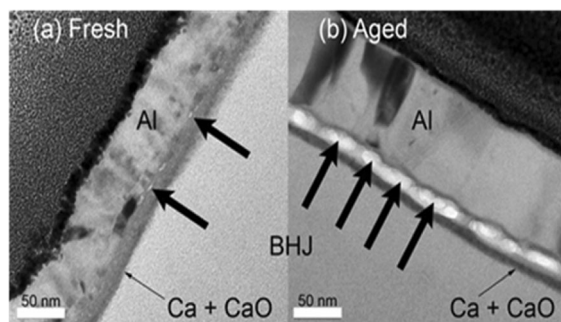
Figure 7. TEM images of a) freshly prepared and b) aged ITO/BHJ/Ca/Al devices. The active organic region is labeled BHJ, the aluminum layer of the electrode is identified as Al, and the calcium layer, which likely contains a significant fraction of calcium oxide, is labeled Ca + CaO. Bold arrows indicate regions of void formation at the Ca/Al interface that enlarge as the devices age. Reprinted with permission from ref. [101].

(TCO) material together with the hole-transport buffer layer on top of the TCO], or the cathode in inverted structures together with an electron-transporting (n-type) oxide or other layer. ITO is the most commonly used material as the TCO in OPV devices, and as mentioned in Section 2.4. of this paper, the most commonly used material for the hole-transport buffer layer is PEDOT:PSS.

For organic light-emitting diodes (OLEDs), it has been observed that the acidity of the PEDOT:PSS layer can cause etching of the indium from the ITO electrode and the liberation of indium ions, which then diffuse throughout the device.[106] This process is accelerated in the presence of moisture.[107] The mechanism of ITO etching by PEDOT:PSS in OPVs has been investigated in detail.[108] According to this degradation mechanism, the excess amount of protons present in the acidic PEDOT:PSS weakens the In—O and Sn—O bonds in ITO by polarization. Free PSS (RSO_3^-) ligands replace the surface water, and then detachment of the PSS–In [$(RSO_3)_3In$] and PSS–Sn [$(RSO_3)_4Sn$] complexes results in stripping of surface In and Sn. XPS analysis has shown that continuous degradation of ITO-based devices results from the continuous migration of indium into the PEDOT:PSS layer.[108] Notably, the approach proposed by Yambem et al.[108] was based on studies in which the etching mechanism was verified only for OLEDs.[107] Thus, due to the different nature of operation of OPVs, the extensive knowledge obtained in OLED applications with regard to degradation of the transparent electrode is of limited help. Furthermore, by studying PEDOT:PSS derivatives with different PH values, Voroshazi et al. demonstrated that the hygroscopic behavior of PEDOT:PSS is responsible for device degradation, not its acidic properties.[96]

3. Recent Advances in Improving the Stability of OPVs

In this section, some of the main methods that have been used in recent years to improve device lifetime are discussed. Given that improvements in any part of an OPV device can lead to increased stability and lifetime, methods for improving

device stability are presented separately for each part of the device. Figure 8 outlines some of the most important advances in improving OPV stability.
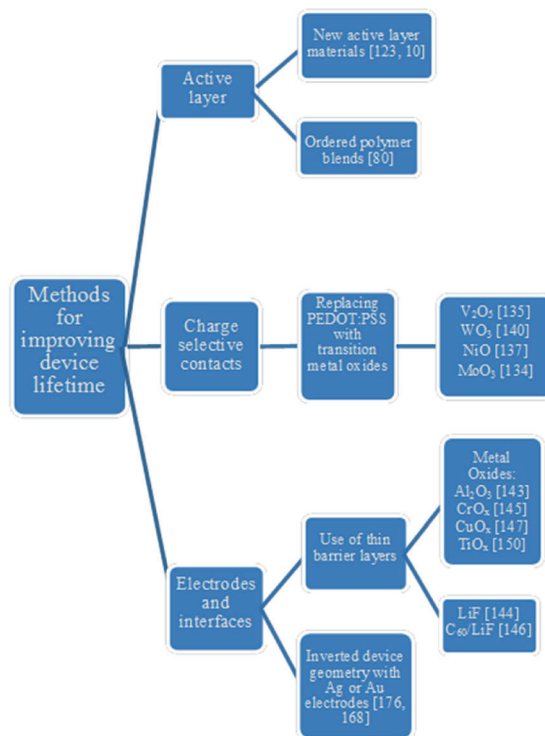
Figure 8. Main methods for improving device lifetime, classified according to the part of the device to which they are applied.

3.1. Active Layer

Most polythiophenes currently used in OPV devices have morphologically stable bulk heterojunctions with regioregular P3HT as the donor material, whereas the soluble PCBM fullerene material is used as the acceptor material. There have been recent attempts to substitute the donor material in OPVs with small-molecule semiconductors such as oligoselenophene derivatives,[109] quinacridones,[110] boron (subphthalocyanine) derivatives,[111] and azadipyrromethenes.[112] Such devices have shown promising results in terms of device efficiency, but their stability has not yet been studied sufficiently.

For more conventional, P3HT:PCBM-based devices, it has been shown[64] that protection from oxygen and water with appropriate encapsulation can lead to a device lifetime of several years under use conditions. Stable device operation for 1000 h has been reported for complete devices by using P3HT:PCBM polymer blends with a LiF/Al cathode,[113] and this has been increased to 5000 h upon using state-of-the-art encapsulation with a cavity glass-on-glass architecture (with a Ca/Al cathode).[114] Another approach for extending the lifetime of OPVs is to use an azide-functionalized graft copolymer of P3HT and polystyrene.[115] These devices are heat treated at 140 °C after preparation to chemically link the active-layer blend components. This approach results in a loss in efficiency of the OPV device but to a considerable increase in its stability. A simple

↖↖ These are not the final page numbers!

and low-costing method to increase stability, and under certain conditions the efficiency, of fullerene-based OPVs has been proposed.[116] It has been observed that exposure of blend polymer:PC$_{60}$BM solar cells to low-level light results in a tenfold increase in device thermal stability due to light-induced oligomerization of PC$_{60}$BM, which hinders diffusion and crystallization in the blend.

Much research effort has been focused on developing new polymers that will enhance the efficiency and stability of solar cells[117] and protect OPVs against degradation due to exposure to high temperatures. In this context, Tromholt et al.[118] have developed a method for reliably assessing the photochemical stability of various organic materials by investigating a wide absorbance range for all samples. Manceau et al.[119] have also investigated the photochemical stability of a large number of polymer donors to establish a set of general rules that connect polymer structure with photochemical stability. They have reported improved stability in thermocleavable polymers and in polymers with aromatic polycyclic units. The photochemical stability of thermocleavable polymers has also been investigated.[120] In this study, several different polymers were subjected to illumination in air, and it was observed that side-chain thermal cleavage led to a strong increase in sample lifetime, as defined by the polymer's ability to absorb light. Although device efficiency for OPVs with thermocleavable donors was found to be relatively low,[121] device half-life exceeded 3900 h under illumination. Several new polythiophene[20] and fullerene[122] derivatives have also shown promising results to date. Certain low-band-gap dithiophene-based polymers have been found to have higher photochemical stability than P3HT,[123] probably due to the presence of fused-ring systems, which are considered to provide higher photochemical stability than thiophene. Helgesen et al.[124] have synthesized low-band-gap dithiophene-based polymers with different bridging atoms and have investigated their photochemical stability. They found that upon subjecting the polymers to illumination in air, substitution of the bridging carbon atom with silicon results in a significant improvement in stability. The performance of bromine-functionalized polythiophene (Br-P3HT) copolymers controlled to achieve a UV-photo-cross-linkable layer[125] has also been investigated. The performance of Br-P3HT:PCBM devices has been compared to that of the corresponding P3HT:PCBM OPVs, and the UV-cross-linked polymers exhibit increased thermal stability. In a different study,[126] four different types of functionalities for cross-linking were assessed. In this case, bromine, azide, vinyl, and oxetane molecules were incorporated into the side chains of a low-band-gap polymer. The cross-linked polymers with bromide and azide links were found to have the highest thermal and morphological stability, but there were no indications of increased photochemical stability. Cross-linking has also been used to create hydrogels by using natural polymers (gelatin and carrageenan).[127] The combination of biochemical and physical cross-linking processes enables the formation of biohydrogels with tunable properties, such as increased mechanical strength and increased thermal stability. Studies of cross-linkable polymers show that there is future potential for designing thermally stable polymers for

OPVs, although efficient encapsulation of the resulting devices would still be required to enhance their photochemical stability.

It has also been reported that a dihexylfluorene-based fullerene derivative (DHFCBM) used as an acceptor in P3HT:DHFCBM OPV devices in optimized concentrations in the active-layer blend increases the thermal stability of the cells if utilized at concentrations between 30 and 50%, as it presents a PCE drop of just 5% after 10 h exposure at 150°C. On the contrary, if used at higher concentrations the drop in PCE is approximately 85 to 90% after 10 h exposure at 150°C. However, this work does not present a comparison with the reference P3HT:PCBM.[128] OPVs using poly[9'-heptadecanyl-2,7-carbazole-alt-5,5-(4',7'-di-2-thienyl-2',1',3'-benzothiadiazole)] (PCDTBT) in the polymer blend together with the fullerene derivative [6,6]-phenyl C$_{70}$-butyric acid methyl ester (PC$_{70}$BM) have also been developed,[129] and they exhibit an efficiency of over 6%.[9] If protected by a glass encapsulant containing a desiccant layer and sealed with a UV epoxy resin, they yield a very high lifetime of approximately 7 years under illumination. Hydrogen bonding of diblock copolymers (Figure 9) has also been known
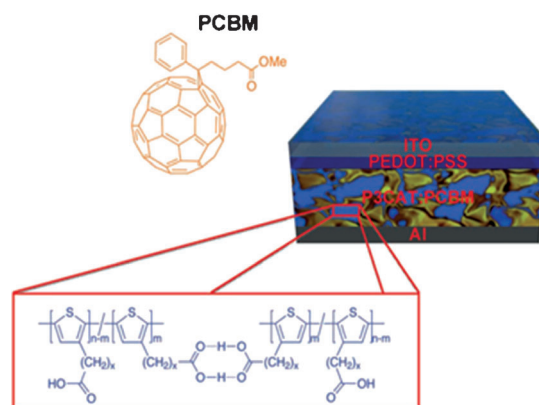
Figure 9. A schematic representation of the OPV device architecture consisting of ITO/PEDOT:PSS/P3CAT:PCBM/Al and depiction of the hydrogen bonding in (P3CATs) poly[3-(carboxyalkyl)thiophene-2,5-diyl]. Reprinted with permission from ref. [130].

to increase device performance (up to 2.6% fabricated in air) and lifetime, as it encourages greater molecular level ordering, increases molecular rigidity, promotes interfacial electron transfer, and reduces charge trap sites, which thus extends device lifetime.[130] Hydrogen bonding has been used to form electron-acceptor domains within a block copolymer self-assembled nanostructure (Figure 10).[80] It has been reported that the thermal stability of the resulting P3HT-block-poly[3-(2,5,8,11-tetraoxadodecane)thiophene] (b-P3TODT)/bis-[6,6]-phenyl-C$_{61}$-butyric acid (bis-PCBA) devices is considerably higher than that of devices based on P3HT/PCBM blends. The P3HT-b-P3TODT/bis-PCBA devices have a PCE reduction of 50% after 6 h at 150°C, whereas devices based on P3HT/PCBM blends present a PCE reduction of 80 to 85% under the same thermal annealing conditions.

These are not the final page numbers! ↗↗
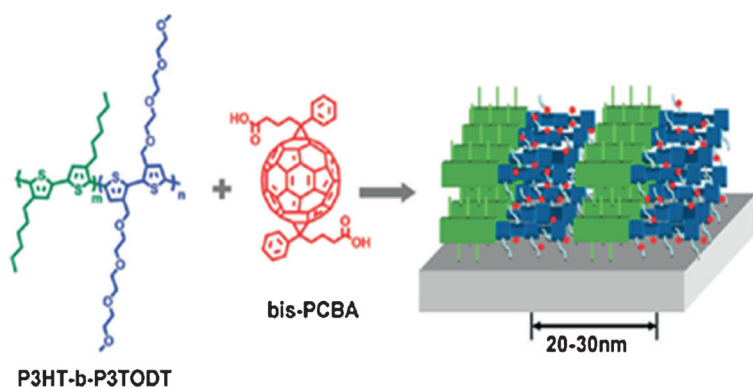
Figure 10. Chemical structures of P3HT-b-P3TODT and bis-PCBA and schematic of the ordered, self-assembled blend that serves as the active layer in the OPV device. Reprinted with permission from ref. [80].

3.2. Charge-Selective Contacts

As mentioned in Section 2.4, PEDOT:PSS, which is commonly used as a hole-transport layer in OPVs, is especially vulnerable to moisture. For that reason, a humidity-insensitive alternative to the PEDOT:PSS layer would help to increase the stability of OPVs. Such an alternative would significantly relax the requirement for water-barrier layers for the encapsulation of organic solar cells, which would thus enable the development of stable organic solar cells on low-costing, flexible substrates.

The influence of different hole-transport layers on device stability has been investigated in an attempt to replace the PEDOT:PSS layer with a more stable material.[131] Three different hole-transporting layers have been tested: PEDOT:PSS (water-based) and polyaniline:poly(styrene sulfonate), both water and isopropyl alcohol (IPA)-based. The stability of solar cells under illumination is lower in devices prepared with water-based layers than in devices prepared with the IPA-based layer due to the existence of additional trap states in water-based layers.

The most promising class of materials for hole transport and electron block in OPVs is transition-metal oxides.[132] Progress in OPV stability has been achieved by using semiconducting metal oxides as charge-extraction interlayers.[133] Both n- and p-type transition-metal oxides with good transparency in the visible and infrared regions make good ohmic contacts to both donors and acceptors in polymer bulk heterojunction solar cells. Their compatibility with roll-to-roll processing makes them very attractive for the cheap manufacture of polymer solar cells. Many transition-metal oxides have been used successfully to replace PEDOT:PSS, such as MoO_3,[134] V_2O_5,[135] WO_3,[136] and NiO.[137] These layers can be deposited by simple and cheap solution processes[138] and have been shown to improve the performances of devices.[139] If a solution-processed WO_3 layer is used to replace PEDOT:PSS (Figure 11),[140] the stability of the resulting OPVs is considerably higher than that with PEDOT:PSS due to the increased air- and photostability of the WO_3 layer.[141] Thermally evaporated WO_3 films have also been used to replace the PEDOT:PSS layer, and power conversion efficiencies that are improved relative to those of PEDOT:PSS-based devices have been reported.[142] Similarly, increased device efficiency and stability have been reported for

poly[2,6-(4,4-bis-(2-ethylhexyl)-4H-cyclopenta[2,1-b;3,4-b']dithiophene)-alt-4,7-(2,1,3-benzothiadiazole)] (PCPDTBT):C_{71}-PCBM OPVs by using NiO and MoO_3 as hole-transporting layers instead of PEDOT:PSS.[142]

3.3. Electrodes and Interfaces

Recent studies have demonstrated that the existence of an ultrathin layer between the metal electrode and the active layer acts as a barrier and prevents the reaction between the metal electrode and the polymer. Al_2O_3,[143] LiF,[144] and CrO_x[99] barrier layers have been successfully used for this purpose. It has also been observed[99] that the oxidation of Al leads to the formation of a charge-blocking layer and that the use of CrO_x as an interfacial layer improves device lifetime by preventing and minimizing
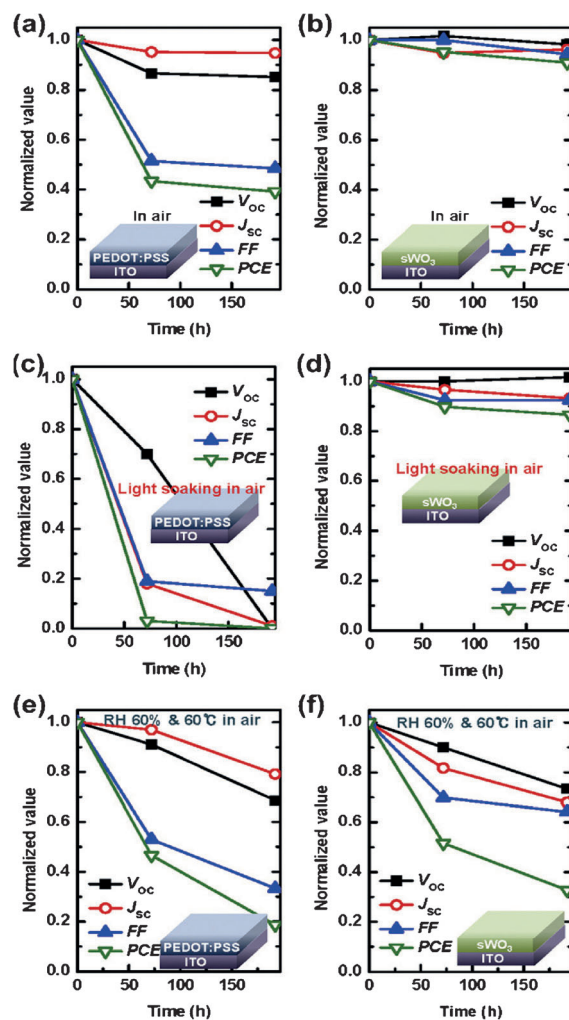
Figure 11. a, b) Cell stability of ITO/HEL/P3HT:PCBM/Al devices by using PEDOT:PSS and WO_3 layers stored in air for 192 h. HEL = hole extraction layer. c, d) Cell stability of ITO/HEL/P3HT:PCBM/Al devices by using PEDOT:PSS and (sWO_3) solution-processed WO_3 layers stored in air under light soaking conditions for 192 h. e, f) Cell stability of ITO/HEL/P3HT:PCBM/Al devices by using PEDOT:PSS and sWO_3 layers stored under a relative humidity of 60% at 60 °C for 192 h. Reprinted with permission from ref. [140].

↖↖ **These are not the final page numbers!**

the formation of an Al–organic interface that is prone to oxidation. P3HT:PCBM devices with and without a CrO_x interfacial layer have been compared,[145] and devices with CrO_x display stability that is more than 100 times higher than that of devices without an interfacial layer. Higher device stability has also been achieved by utilizing other barrier interfaces such as C_{60}/LiF,[146] CuO_x,[147] C_6H_5COOLi,[148] and Cs_2CO_3.[149] Another material that is commonly used as a protective layer is TiO_x, the deposition of which on top of the active layer has been observed to increase device stability[150] by preventing oxygen and humidity from entering the active layer.[151]

In general, the utilization of barrier interfaces on the upper and lower surfaces of the active layer isolates the active layer, which prevents penetration of oxygen and humidity and ultimately reduces degradation of the active layer. Moreover, metal-oxide interfacial layers tend to create bonds with atmospheric oxygen, which thus protects the metal electrode from oxidation.[150] Hydroxy groups and −OR functionalities within the oxide are activated with UV radiation and are photooxidized, which consumes O_2 and produces CO_2 and H_2O in the form of gas. The photoactivation of these films leads to O_2 scavenging and opens new horizons for thin films, which trap oxygen upon exposure to light.[150]

In addition, it has been observed that poor adhesion between device layers may result in a loss of device performance from delamination driven by the thermomechanical stresses in the device.[152] A thin-film adhesion technique by using postdeposition annealing can be applied to flexible OPVs to increase adhesion between layers.[153]

Metal electrodes that yield high stability have also been produced by using various printing techniques for devices with normal[154] and inverted[155] architecture, as well as for tandem OPVs.[156] Yu et al.[157] have used different printing techniques to produce bottom Ag electrodes for P3HT:PCBM OPVs. They compared hexagonal silver grids prepared by using either roll-to-roll inkjet or roll-to-roll flexographic printing with a roll-to-roll thermally imprinted grid that was filled with silver. They observed that the embedded grid and the flexographic grid performed equally well, but the flexographic technique allowed faster processing and lower silver use, and the embedded grid presented higher optical transparency and conductivity. Inkjet printing has also been used[155] to produce solution-processed top electrodes for inverted P3HT:PCBM OPVs with a power conversion efficiency in the vicinity of 3%. A mixture of Ag nanoparticle inks was developed in this case to control the printability and electrical conductivity of the electrodes.

The main advantages of using printing techniques for OPVs is the ability to develop flexible, large-scale modules with long operating lifetimes.[158] Krebs et al.[159] have used screen printing to produce silver back electrodes for roll-to-roll-processed OPVs comprising thousands of discrete miniature devices. Similarly,[160] they also produced fully printed P3HT:PCBM OPVs with printed Ag electrodes. After 1 year of outdoor testing, these encapsulated devices maintained 95% of their initial performance. Sommer-Larsen et al.[161] demonstrated that large-scale P3HT:PCBM OPVs with Ag back electrodes can be fully printed on flexible substrates by using roll-to-roll processes.

More recently,[154] roll-to-roll processes to print Ag back electrodes were used for a large number (hundreds of thousands) of serially connected P3HT:PCBM OPVs. These devices were used for a solar park installation, and after an initial drop in performance ($\approx 20\%$), they exhibited high operational stability in outdoor conditions.

In addition, roll-to-roll processes have been used successfully to produce ITO- and Ag-free electrodes. In a recent study,[162] silver was replaced with carbon as the electrode material, and it was observed that substitution of silver with carbon did not affect the roll-to-roll process and allowed for the same fast printing and coating. In the same study, it was reported that the replacement of Ag electrodes with C ones lowered the manufacturing costs of OPVs but their flexibility, efficiency, and stability were retained. Larsen-Olsen et al.[163] also used roll-to-roll processes to replace Ag with C as the back electrode in P3HT:PCBM OPVs. They observed that the performance of the modules is similar to that of ITO-based devices, whereas there is a cost reduction by a factor of >10 and an increase in processing speed by a factor of >10.

3.4. Inverted Structured OPVs

OPVs with an inverted structure have shown promise for higher lifetimes than those with a normal structure mainly because some of the mechanisms responsible for the degradation of OPVs do not exist if the cell structure is inverted.[164] In inverted device geometries, the two electrodes are essentially reversed, and electrons flow from the back electrode to the transparent electrode, which allows the use of a solution-processed back electrode.[94] Figure 12 shows a comparison between typical normal and inverted device structures.

The inverted cell structure is more stable than the normal structure mainly because the reaction between the metal electrode and the polymer (oxidation and chemical reaction) is prevented. The PEDOT:PSS interface is also moved on the top electrode, and thus, interfaces become modified (Figure 12). Thus, the inverted cell configuration leads to improved device lifetime by increasing cell protection against oxygen and moisture damage.[165] Devices with an inverted structure have been shown to have higher stability than those with a normal structure, particularly if Ag or Au is used as the top electrode.[166] Ag and Au are high work function metals and are more resistant to oxidation than Al,[99] and this leads to improved device stability.

It has been shown that a nonencapsulated, inverted P3HT:PCBM cell can retain over 80% of its original efficiency after 40 days in air, whereas a corresponding normal cell lasts less than 4 days under the same environmental conditions.[167] Similarly, the stability of nonencapsulated bulk heterojunction (BHJ) devices of normal and inverted structures has been compared, and the efficiency of inverted cells is much higher after 40 days of exposure in air than that of corresponding normal cells (Figure 13).[168] It has also been reported that encapsulated, inverted P3HT:PCBM OPVs retain approximately 96% of their efficiency after 120 h of continuous irradiation[133] and that inverted OPVs degrade more slowly under high humidity

These are not the final page numbers! ↗↗
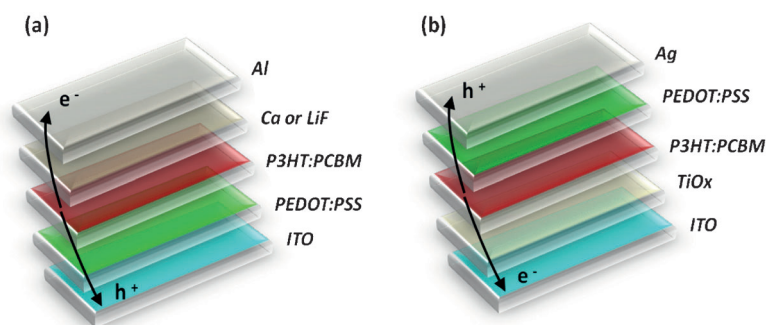
Figure 12. Typical a) normal and b) inverted device architectures. The normal OPV is based on ITO/PEDOT:PSS/semiconductor (SC) blend/metal and the inverted OPV is based on ITO/TiO$_x$/SC blend/PEDOT:PSS/metal.
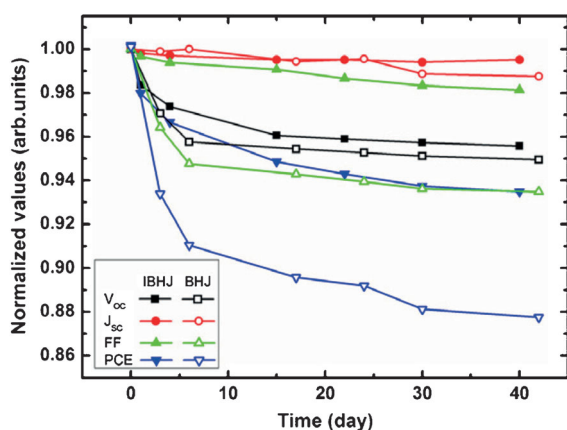
Figure 13. Plot of solar-cell parameters as a function of time in ambient air. Solid symbols represent the parameters of BHJ inverted solar cells and open symbols represent those of conventional BHJ solar cells. Reprinted with permission from ref. [168].

conditions than the corresponding cells of the normal structure.[169]

In addition, comparative studies between normal and inverted devices that utilize PEDOT:PSS as a hole-selective contact have shown that although inverted structures have longer lifetimes, the hygroscopic nature of PEDOT:PSS causes serious degradation problems.[96] The phase separation of PEDOT:PSS as well as its interaction with the active layer are considered to be the main causes of PEDOT:PSS-induced degradation.[82, 32] A decrease in the electrical conductivity due to water absorption has also been reported.[91, 92, 94, 95] Another study that compares inverted and normal OPV structures under heat reports higher stability of inverted structures due to electron-barrier formation in normal OPV geometries.[85]

Several research efforts have focused on improving the efficiency and stability of inverted OPVs. In a process similar to the one described in Section 3.2 for OPVs with a normal structure, the unstable PEDOT:PSS layer in inverted OPVs can be replaced by a transition-metal oxide layer. Efficient inverted solar cells with a V$_2$O$_5$ anode buffer layer have been developed,[170] and OPV devices with such a V$_2$O$_5$ anode layer have a longer shelf life than devices with a PEDOT:PSS layer.[171] Furthermore, the efficiency and thermal stability of inverted OPVs with a va-

nadium oxide anode layer are improved relative to the same parameters of the corresponding devices with a PEDOT:PSS anode layer.[172] Other buffer layers, such as Ti or Cr, have been used, and the use of Cr considerably increases the stability of the devices under illumination.[173] CuO$_x$ layers have also been used at the anode of inverted P3HT:PC$_{61}$BM OPVs, and the presence of the CuO$_x$ layer increases device efficiency and stability compared to corresponding devices without an interlayer, which demonstrates that the CuO$_x$ layer can provide protection from oxygen and moisture to the active layer.[174]

Finally, a metal-oxide (e.g. TiO$_x$,[175] ZnO,[167] Al$_2$O$_3$[176]) layer can be used at the cathode of inverted cells to improve electron extraction and device stability.[177] Cs$_2$CO$_3$ layers have been used at the inverted OPV cathode and MoO$_3$ layers have been used at the anode, and it has been reported that the lifetime performance of these cells is improved relative to that of the corresponding cells with a conventional PEDOT:PSS layer.[168]

4. Low-Cost Encapsulation

The quality and type of encapsulation play an important role in the stability and overall lifetime of the device by limiting the amount of oxygen and water molecules that permeate the device as well as preventing UV exposure through the utilization of UV-filtering encapsulation. UV-blocking layers can increase the long-term stability of organic solar-cell devices by filtering out UV radiation.[178] TiO$_x$ layers have been used effectively as UV-blocking layers in P3HT:PCBM inverted organic OPVs, and device stability increases with increasing TiO$_x$ film thickness.[179] In P3HT:PCBM devices with a normal architecture, TiO$_2$–SiO$_x$ layers have been successfully used to block UV radiation.[180] In the same work, a luminescent layer was also inserted on top of the UV-blocking layer to enable photon recycling, which thus enhanced device performance.

There are many different materials that can be used to encapsulate OPVs, and they vary considerably in both effectiveness and cost. To keep production costs of OPVs as low as possible, it is important to use low-costing packaging materials, but usually an optimum balance is sought between the effectiveness of the packaging materials and their cost. It is therefore important to develop new encapsulation techniques that improve device stability and that are compatible with device flexibility and a low cost of fabrication at the same time.

Several encapsulation studies over the past few years have shown that the shelf life of OPVs can be extended to many thousands of hours by using appropriate encapsulation materials, both flexible[22] and rigid.[77] The ability of oxygen and moisture to pass through an encapsulating membrane is represented by the oxygen transmission rate (OTR) and the water vapor

transmission rate (WVTR), respectively.[181] The WVTR of OLEDs with a lifetime over 10 000 h is 1×10^{-6} g m^{-12} day^{-1}. OPV barrier requirements are believed to be less stringent[182] with a WVTR of 1×10^{-3} g m^{-12} day^{-1} to be sufficient for the protection of OPVs against atmospheric agents.[169] As shown in Figure 14, the requirements for organic electronic devices are considerably higher than the WVTR barriers provided by commercial sealants and so new technologies have to be developed.[183]
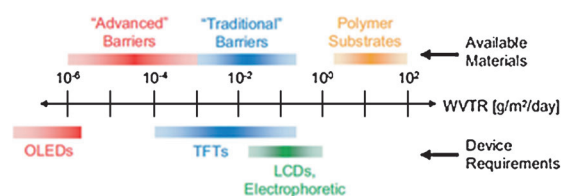
Figure 14. WVTR requirements for common flexible electronic devices and the barrier performance provided by available materials. Reprinted with permission from ref. [183].

One of the simplest packaging options available is to cover the device with glass plates and to use an epoxy-type sealant to hold them in place.[184] This configuration provides the device with effective protection against oxygen and moisture, but it is not suitable for the production of flexible devices. Given that flexibility is one of the key advantages of OPVs,[185] several research efforts have been focused on developing an encapsulation material that will be flexible and at the same time have all the above advantages, that is, adequate protection to the device, transparency, and low cost. Figure 15 a shows a schematic design of an OPV encapsulated in a flexible substrate, whereas Figure 15 b shows a picture of the final flexible device.[186]
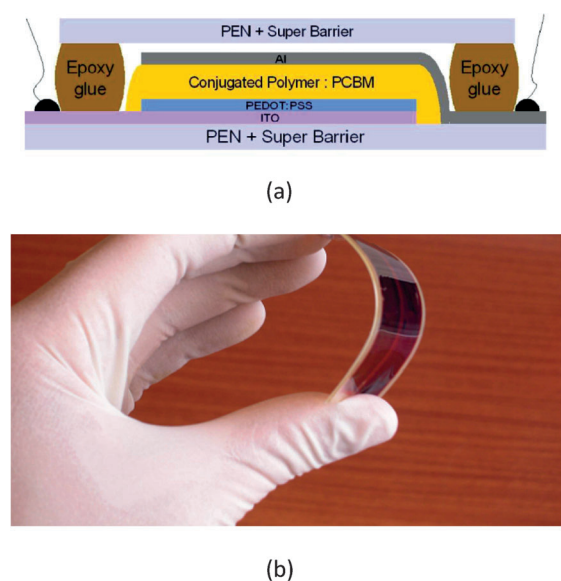
Figure 15. a) Cross-sectional view of the conjugated polymer:fullerene solar cells with a flexible barrier; b) picture of a bent device. Reprinted with permission from ref. [186].

Several inorganic materials have been used for encapsulating solar cells with varying degrees of success. Single-layer, silicon-based dielectric films deposited by plasma-enhanced chemical vapor deposition have been used as encapsulating materials,[187] and their oxygen and water transmission rates have been studied.[188] However, the effectiveness of these materials for encapsulation has been proven to be rather limited (OTR values of ≈ 0.5 mL m^{-2} day and WVTR of ≈ 0.3 g m^{-12} day have been measured) and the cost of the encapsulation process would be relatively high in this case. Thin oxide films such as TiO_2 and Al_2O_3 have also been used, although these films are still permeable to some degree by water molecules, mainly due to pinhole defects or to the existence of pores on their surface.[189] Al_2O_3 films deposited by atomic layer deposition (ALD) have been used, either on their own or in combination with a UV sealant for pentacene/C_{60}-based solar cells.[190] The single Al_2O_3 layer was found to be the most effective sealant, as it prevents cell degradation to a large degree—only 6% loss after over 6000 h exposure to ambient (but not accelerated) atmospheric conditions. More recently, ultrathin Al_2O_3 layers have been used as encapsulation barriers for P3HT:PCBM OPVs, deposited by a different ALD method.[191] In that study, H_2O was replaced with O_3 as the ALD oxidant, and the Al_2O_3 layers deposited by using O_3 displayed superior device encapsulation than films deposited by using H_2O; they retained 80% of their efficiency after 500 h in air. However, the use of an ALD technique may not be practical for large-scale commercial applications, mainly due to the long times required for film development. Also, prolonged heating of the devices at high temperatures (over 100 °C), required for encapsulating the devices, may increase device degradation.[191]

Various polymer composites have also been used as OPV encapsulants, such as polyisobutene[192] and ethylene vinyl acetate (EVA).[193] Those preliminary works reported improved device stability with the use of encapsulants, and in the second case, the EVA material was subjected to a wide range of temperatures, but detailed aging and lifetime studies of the OPV devices were not conducted to determine the efficacy of the materials as encapsulants for such devices.[194] A polymer encapsulant for OPV devices has also been developed by using polymer nanotube composites based on a copolymer of vinylidene chloride and acrylonitrile.[8] The effectiveness of such sealants has been tested on P3HT films, and the encapsulants provide effective protection against atmospheric degradation and have excellent transparency in the visible region and good thermal stability.[8] These results are promising for OPV applications, but the degradation of complete devices encapsulated with this material has not been investigated to date.

Flexible P3HT:PCBM modules have also been encapsulated by using commercial barrier foil, and average efficiencies of approximately 40% of the original values have been observed after approximately 1000 h of outdoor exposure.[194] ITO-free inverted OPVs with Cr/Al/Cr as a bottom electrode and a metal grid on top have been encapsulated by using commercial barrier foils and have been found to exhibit a lifetime of more than 1000 h under damp-heat accelerated lifetime conditions.[195] Polyurethane has also been used to encapsulate in-

These are not the final page numbers! ↗↗

verted OPVs with P3HT:PCBM as well as commercial active-layer materials, and cells encapsulated with polyurethane retain on average 40% of their efficiency after more than 3000 h of outdoor exposure.[196] In another study, nonencapsulated cells have been tested and compared with cells protected by using three different encapsulation methods: an inorganic SiO_x film, an organic layer of Kapton tape (polyimide film with silicone adhesive), and a glass/thermoplastic layer.[197] All of the encapsulation methods have been shown to improve the stability of the device, and films encapsulated with the inorganic SiO_x film lost the smallest percentage of their original efficiency over time.

Most organic films used for encapsulation can be considered homogeneous with regard to their thicknesses, whereas inorganic films tend to have more defects and irregularities. Hybrid inorganic/organic films utilize the properties of both inorganic and organic materials to achieve ultrahigh barrier properties. These films are structured as multilayer stacks comprising inorganic oxide layers separated by polymer layers. Inorganic layers have high intrinsic barrier properties, whereas the organic layers give more flexibility to the final material and eliminate some of the defects that cause water permeation in inorganic materials. An added advantage is that these films can be developed by using roll-to-roll processes. Hybrid Al_2O_3/polyethylene terephthalate (PET) films with excellent barrier properties have been developed,[198] and a method to assess the properties of such films has been proposed.[89] Attempts to create flexible packaging for various organic devices by using such a hybrid multilayer barrier have been reported elsewhere with promising results.[199, 200]

The aforementioned hybrid ultrahigh barrier materials have also been used in OPVs and have shown excellent protective abilities against atmospheric agents. Flexible poly(ethylene naphthalate) (PEN) substrates have been used, coated with ultrahigh barrier foils, and sealed with epoxy resin.[186] The ultrahigh barrier coatings were made from alternating layers of inorganic (SiO_x) material and plasma-deposited organic material (organosilicon) sealed together with an epoxy resin, and shelf lifetimes over 3000 h have been reported for MDMO-PPV:PCBM devices sealed with this material.[201] This work has been continued in another study, in which flexible encapsulants (the same PEN substrates with ultrahigh barrier as described above) have been compared with rigid ones (glass slides) for large-area (MDMO:PPV):PCBM and P3HT:PCBM OPVs connected in series.[22] It was observed that the efficiency of the cells with flexible foils was lower than that of cells with a rigid encapsulant. However, the stability of the cells encapsulated with the flexible material was found to be considerably high and a 6000 h shelf lifetime (50% of original efficiency) was recorded for the P3HT:PCBM flexible devices.[22] A comparative assessment of various sealants for small-molecule organic solar cells has also been conducted.[87] In that study, organic (PET) and organic/inorganic (zinc tin oxide on PET substrates) encapsulants were compared with a glass packaging sealed with a UV-activated epoxy resin. The glass encapsulant was found to provide the best protection against water permeation, whereas one of the organic/inorganic encapsulants yielded the second-best

performance; this demonstrated the efficacy of the hybrid materials as flexible sealants for OPV devices. Multilayer barriers of parylene and aluminum oxide coatings have also been shown to provide P3HT:PCBM-based OPV devices with good protection from atmospheric agents for several hours under illumination (lifetime was three times higher in the presence of a multilayer barrier),[202] and such coatings successfully protect P3HT layers from atmospheric degradation.[203] Notably, however, even though the organic encapsulants are not as effective in sealing the device as glass or hybrid barriers, they are more flexible than the glass ones and they also have a lower cost than the hybrid barriers.

One common issue with the epoxy resins often used to seal the devices is that they may contain trace amounts of moisture or oxygen unless a degassing process is performed. To eliminate trace amounts of moisture, a getter sheet can be included on the inside of the packaging layer.[204] There is a wide variety of getter materials that can be used for this purpose, including zeolite in various forms, oxides such as BaO and CaO, and reactive metals such as Ba and CaO nanoparticles.[205] Highly transparent and easy-to-process liquid getters have also been developed. The effectiveness of glass encapsulants with and without a liquid-getter-filled barrier has been compared,[206] and the barrier properties of the liquid-getter-filled encapsulation are comparable to those of the conventional glass encapsulation and gives the advantage of improved thermal properties. Promising results have also been reported for inverted OPVs with glass encapsulation that includes a getter layer to ensure that a minimum amount of water molecules remain inside the device, and a comparative assessment of the lifetime of inverted P3HT:PCBM OPVs with and without encapsulation has been conducted.[207] The packaging in that case was achieved with a glass plate with a water getter sheet coated by an epoxy-UV resin as the sealing material. The encapsulation increased the lifetime of the device from 20 h to well over 120 h (the device was operating at 96% of its efficiency at the time) under illumination. Large-area (233 cm^2) P3HT:PCBM OPV modules have also been produced and sealed with a glass sheet and getter encapsulation system; the lifetime of these systems under illumination was estimated to be over 5000 h.[26] By using a similar type of encapsulation, a lifetime approaching seven years under illumination has been achieved for PCDTBT/$PC_{70}BM$ OPV devices.[129] Recently, Adams et al.[208] designed a P3HT:PCBM/diketopyrrolopyrrole-quinquethiophene (pDPP5T-2):$PC_{70}BM$ organic tandem solar cell with an inverted device geometry. The cell was sealed with a glass encapsulant and a UV-curable epoxy resin. After 2000 h under illumination, the device retained 89% of its efficiency. By extrapolating this value to 80% of the initial PCE, an accelerated lifetime of >10 years can be estimated.

Even though providing an impermeable barrier against water and oxygen is crucial to the performance of OPV devices, the ease and cost of the encapsulation process are, in the end, the most important parameters in choosing encapsulating materials. Recent studies have shown that commercial PET films can be easily deposited on P3HT:PCBM OPVs by using a roll-to-roll process, and they provide adequate protection

↖↖ These are not the final page numbers!

Table 3. Stability of OPV devices achieved with various encapsulation methods.

Encapsulation	Aging method	Efficiency remaining [%]	Time of aging [h]	OPV type
Al_2O_3 film[180]	shelf lifetime	94	6000	pentacene:PCBM
Al_2O_3 film[181]	shelf lifetime	80	500	P3HT:PCBM
commercial barrier foil[53]	outdoor	40	1000	P3HT:PCBM
polyurethane[186]	outdoor	40	over 3000	inverted P3HT:PCBM
inorganic/organic[22]	shelf lifetime	50	6000	P3HT:PCBM
glass sheet[207]	illumination	96	120	inverted P3HT:PCBM
glass sheet[26]	illumination	50	5000	P3HT:PCBM
glass sheet[129]	illumination	80	4000	$PCDTBT/PC_{70}BM$ and P3HT:PCBM
PET with side protection[210]	illumination	almost 100	800	P3HT:PCBM
glass sheet[149]	illumination	over 50	4700	inverted P3HT:PCBM
glass sheet[208]	illumination	89	2000	inverted tandem $P3HT:PCBM/pDPP5T-2:PC_{70}BM$

against atmospheric agents to the devices.[209] This process allows for the production of large-scale flexible OPV devices with longer lifetimes than nonencapsulated devices. The above process has been enhanced by not only covering the device with a polymer layer, but also by adding protection to the sides through an additional encapsulation step.[210] It has been shown that sealing the edges of the device considerably increases its stability and that edge-sealed devices have almost constant efficiency for over 1000 h of operation under illumination.[210] OPVs have also been printed directly on barrier foil and encapsulated with the same barrier foil.[211] In that case, three different adhesives were used to seal the solar cells: pressure-sensitive adhesive, UV-curable glue, and hotmelt. It was observed that single-sided lamination with UV-curable epoxy resin achieved the best-performing encapsulation over a test period of 900 h and presented the additional advantages of being a low-costing and relatively fast encapsulation process. Krebs et al.[212] also printed OPVs directly on barrier foil by employing a newly designed front electrode grid. They achieved efficient edge sealing by printing a UV-curable adhesive on the encapsulation barrier foil and later pierced the devices to allow access to the electrodes. This method is fast and low costing, and the resulting devices are expected to have high stability and prolonged lifetimes.[212]

P3HT/PCBM devices utilizing an inverted architecture have also been shown to retain more than 50 % of their initial efficiency after 4700 h of continuous exposure to 1 sun intensity at elevated temperatures.[173] Table 3 summarizes some of the highest device lifetimes reported achieved with various encapsulation methods. Many of these results are not readily comparable, as they refer to different OPV technologies and aging methods, but they can provide an indication of the device lifetimes achieved with various encapsulation methods. From this table, it appears that cells encapsulated by using glass slides have the longest lifetimes under illumination under accelerated aging conditions.

5. Conclusions

The performance of organic photovoltaic (OPV) devices has considerably improved in recent years, especially in terms of their power conversion efficiency. The lifetime of OPVs has also

increased, but additional efforts are required to produce devices with high stability at low cost.

Advanced characterization studies have been used to confirm and identify the main degradation mechanisms of OPVs, and ISOS protocols are recommended to determine lifetime performance of OPV devices and modules. Several studies have reported favorable progress towards the understanding of degradation mechanisms under different environmental conditions, such as light, moisture, oxygen, and heat. This understanding has led to the development of new materials and device structures that have been efficiently used to limit OPV degradation and improve device lifetime. Major breakthroughs that have led to improved device stability were discussed in this review, including inverted OPV device structures, the use of more photostable active-layer materials, and the introduction of interfacial or buffer layers for device performance optimization.

Moreover, methods for protecting OPVs have been developed that concentrate on sealing the device from various environmental agents. These encapsulation techniques have led to the development of OPV devices with increased stability and lifetime. The product development targets of OPVs, however, demand flexibility and low-costing encapsulation as well. In this review, we examined a number of different packaging options in terms of their ability to protect the device but also in terms of their functionality and overall cost effectiveness. It was discussed that the most effective sealing of the device comes with the cost of high price or loss of flexibility. Although there are a number of low-costing, flexible options that provide adequate protection to the device, a deeper understanding of the degradation parameters is required to provide material design rules and device engineering concepts towards low-costing and long-lived flexible OPVs.

Acknowledgements

These are not the final page numbers! ↗↗

[1] A. Moliton, J. M. Nunzi, *Polym. Int.* **2006**, *55*, 583–600.

[2] J. Nelson, *Curr. Opin. Solid State Mater. Sci.* **2002**, *6*, 87–95.

[3] A. Jager-Waldau, *PV Status Report 2005*, Institute for Environment and Sustainability, European Commission, **2005**.

[4] S. E. Shaheen, D. S. Ginley, G. E. Jabbour, *Mater. Res. Bull.* **2005**, *30*, 10–15.

[5] C. N. Hoth, P. Schilinsky, S. A. Choulis, C. J. Brabec, *Nano Lett.* **2008**, *8*, 2806–2813.

[6] J. Alstrup, M. Jørgensen, A. J. Medford, F. C. Krebs, *ACS Appl. Mater. Interfaces* **2010**, *2*, 2819–2827.

[7] F. C. Krebs. K. Norrman, *ACS Appl. Mater. Interfaces* **2010**, *2*, 877–887.

[8] J. Ravichandran, A. G. Manoj, J. Liu, I. Manna, D. L. Carroll, *Nanotechnology* **2008**, *19*, 085712.

[9] Y. Liang, D. Feng Y. Wu, S. T. Tsai, G. Li, C. Ray, L. Yu, *J. Am. Chem. Soc.* **2009**, *131*, 7792–7799.

[10] S. H. Park, A. Roy, S. Beaupre, S. Cho, N. Coates, J. S. Moon, D. Moses, M. Leclerc, K. Lee, A. J. Heeger, *Nat. Photonics* **2009**, *3*, 297–302.

[11] Y. Liang, Z. Xu, J. Xia, S. T. Tsai, Y. Wu, G. Li, C. Ray, L. Yu, *Adv. Mater.* **2010**, *22*, 135–138.

[12] T. Wemett, *Konarka's Power Plastic Achieves World-Record 8.3% Efficiency, Certification from National Renewable Energy Laboratory (NREL)*, Konarka Technologies, Inc., Lowell, MA, **2010**; available online: http://www.konarka.com/index.php/site/pressreleasedetail/konarkas power plastic achieves world record 83 efficiency certification fr.

[13] Z. He, C. Zhong, S. Su, M. Xu, H. Wu, Y. Cao, *Nat. Photonics* **2012**, *6*, 591–595.

[14] P. Clarke, *Heliatek Pushes Organic Solar Cell Efficiency Higher*, EE Times **2012**; available online: http://www.eetimes.com/electronics-news/4371884/Heliatek-pushes-organic-solar-cell-efficiency-higher.

[15] T. Nozawa, *Mitsubishi Chemical Claims Efficiency Record for Organic Thin-film PV Cell*, Nikkei Electronics, **2012**; available online: http://techon.nikkeibp.co.jp/english/NEWS EN/20120601/221131/.

[16] Heliatek press release, *Heliatek Consolidates its Technology Leadership by Establishing a New World Record for Organic Solar Technology with a Cell Efficiency of 12%*, **2013**; available online: http://www.heliatek.com/newscenter/latestnews/neuer-weltrekord-fur-organische-solarzellen-heliatek-behauptet-sich-mit-12-zelleffizienz-als-technologiefuhrer/?lang=en.

[17] Y. Liu, C. C. Chen, Z. Hong, J. Gao, Y. M. Yang, H. Zhou, L. Dou, G. Li, Y. Yang, *Sci. Rep.* **2013**, *3*, 3356.

[18] National Renewable Energy Laboratory (NREL), Golden, CO, **2014**, http://www.nrel.gov/ncpv/

[19] F. C. Krebs, K. Norrman, *Prog. Photovoltaics* **2007**, *15*, 697–712.

[20] L. Yang, S. K. Sontag, T. W. LaJoie, W. Li, N. E. Huddleston, J. Locklin, W. You, *ACS Appl. Mater. Interfaces* **2012**, *4*, 5069–5073.

[21] M. Jørgensen, K. Norrman, S. A. Gevorgyan, T. Tromholt, B. Andreasen, F. C. Krebs, *Adv. Mater.* **2012**, *24*, 580–612.

[22] C. Lungenschmied, G. Dennler, H. Neugebauer, N. S. Sariciftci, M. Glatthaar, T. Meyer, A. Meyer, *Sol. Energy Mater. Sol. Cells* **2007**, *91*, 379–384.

[23] R. S. Claasen, B. L. Butler, "Introduction to Solar Materials Science" in *Solar Materials Science* (Ed.: L. E. Murr), Academic Press, New York **1980**, pp. 3–51.

[24] O. Haillant, *Sol. Energy Mater. Sol. Cells* **2011**, *95*, 1284–1292.

[25] M. A. Green, K. Emery, Y. Hishikawa, W. Warta, *Prog. Photovoltaics* **2009**, *17*, 320–326.

[26] N. Grossiord, J. M. Kroon, R. Andriessen, P. W. Blom, *Org. Electron.* **2012**, *13*, 432–456.

[27] F. C. Krebs, T. D. Nielsen, *Energy Environ. Sci.* **2010**, *3*, 512–525.

[28] T. D. Nielsen, C. Cruickshank, S. Foged, F. C. Krebs, *Sol. Energy Mater. Sol. Cells* **2010**, *94*, 1553–1571.

[29] C. J. Brabec, *Sol. Energy Mater. Sol. Cells* **2004**, *83*, 273–292.

[30] F. C. Krebs, *Sol. Energy Mater. Sol. Cells* **2009**, *93*, 465–475.

[31] F. C. Krebs, O. Hagemann, T. D. Nielsen, *Sol. Energy Mater. Sol. Cells* **2009**, *93*, 422–441.

[32] F. Krebs, S. Gevorgyan, J. Alstrup, *J. Mater. Chem.* **2009**, *19*, 5442–5451.

[33] F. Krebs, T. Tromholt, M. Jørgensen, *Nanoscale* **2010**, *2*, 873–886.

[34] B. Azzopardi, C. J. M. Emmott, F. C. Krebs, *Energy Environ. Sci.* **2011**, *4*, 3741–3753.

[35] F. Machui, N. Li, G. D. Spyropoulos, T. Ameri, R. R. Søndergaard, D. Gaiser, D. Lenssen, N. Lemaitre, S. Nordman, C. J. Brabec, F. C. Krebs, *Energy Environ. Sci.* **2014**, *7*, 2792–2802.

[36] F. C. Krebs, *Org. Electron.* **2009**, *10*, 761–768.

[37] J. Kalowekamo, E. Baker, *Sol. Energy* **2009**, *83*, 1224–1231.

[38] K. Zweibel, *The Terawatt Challenge for Thin Film PV*, **2005**, Technical Report NREL/TP-520–38350.

[39] K. Kawano, R. Pacios, D. Poplavskyy, J. Nelson, D. D. C. Bradley, J. R. Durrant, *Sol. Energy Mater. Sol. Cells* **2006**, *90*, 3520–3530.

[40] R. de Bettignies, F. Leroy, M. Firon, C. Sentein, *Synth. Met.* **2006**, *156*, 510–513.

[41] S. Bertho, G. Janssen, T. J. Cleij, B. Conings, W. Moons, A. Gadisa, J. D. Haen, E. Goovaerts, L. Lutsen, J. Manca, D. Vanderzande, *Sol. Energy Mater. Sol. Cells* **2008**, *92*, 753–760.

[42] J. Morgado, R. H. Friend, F. Cacialli, *Synth. Met.* **2000**, *114*, 189–196.

[43] D. Sutherland, J. Carlisle, P. Elliker, G. Fox, T. Hagler, I. Jimenez, H. Lee, K. Pakbaz, L. Terminello, S. Williams, F. Himpsel, D. Shuh, W. Tong, J. Lia, T. Callcott, D. Ederer, *Appl. Phys. Lett.* **1996**, *68*, 2046–2048.

[44] L. Do, E. Han, Y. Nidome, M. Fujihira, T. Kanno, S. Yoshida, A. Maeda, A. Ikushima, *J. Appl. Phys.* **1994**, *76*, 18–5121.

[45] C. J. Brabec, A. Cravino, D. Meissner, N. Sariciftci, M. Rispens, L. Sanchez, J. Hummelen, T. Fromherz, *Thin Solid Films* **2002**, *403–404*, 368–372.

[46] M. Schaer, F. Nuesch, D. Berner, W. Leo, L. Zuppiroli, *Adv. Funct. Mater.* **2001**, *11*, 116–121.

[47] K. Norrman, S. A. Gevorgyan, F. C. Krebs, *ACS Appl. Mater. Interfaces* **2009**, *1*, 102–112.

[48] A. Liu, S. Zhao, S. B. Rim, J. Wu, M. Koonemann, P. Erk, P. Peumans, *Adv. Mater.* **2008**, *20*, 1065–1070.

[49] M. Jørgensen, K. Norrman, F. C. Krebs, *Sol. Energy Mater. Sol. Cells* **2008**, *92*, 686–714.

[50] M. V. Madsen, T. Tromholt, K. Norrman, F. C. Krebs, *Adv. Energy Mater.* **2013**, *3*, 424–427.

[51] T. Tromholt, F. C. Krebs, *Sol. Energy Mater. Sol. Cells* **2011**, *95*, 1308–1314.

[52] D. M. Tanenbaum, M. Hermenau, E. Voroshazi, M. T. Lloyd, Y. Galagan, B. Zimmermann, M. Hösel, H. F. Dam, M. Jørgensen, S. Gevorgyan, S. Kudret, W. Maes, L. Lutsen, D. Vanderzande, U. Wurfel, R. Andriessen, R. Rosch, H. Hoppe, G. Teran-Escobar, M. Lira-Cantu, A. Rivaton, G. Y. Uzunoglu, D. Germack, B. Andreasen, M. V. Madsen, K. Norrman, F. C. Krebs, *RSC Adv.* **2012**, *2*, 882–893.

[53] M. O. Reese, S. A. Gevorgyan, M. Jørgensen, E. Bundgaard, S. R. Kurtz, D. S. D. C. Ginley, M. T. Olson, P. Lloyd Morvillo, E. A. Katz, A. Elschner, O. Haillant, T. R. Currier, V. Shrotriya, M. Hermenau, M. Riede, K. R. Kirov, G. Trimmel, T. Rath, O. Inganas, F. Zhang, M. Andersson, K. Tvingstedt, M. Lira-Cantu, D. DarinLaird, C. McGuiness, S. J. Gowrisanker, M. Pannone, M. Xiao, J. Hauch, R. Steim, D. M. DeLongchamp, R. Rosch, H. Hoppe, N. Espinosa, A. Urbina, G. Y. Uzunoglu, J.-B. Bonekamp, A. J. J. M. van Breemen, C. Girotto, E. Voroshazi, F. C. Krebs, *Sol. Energy Mater. Sol. Cells* **2011**, *95*, 1253–1267.

[54] B. Andreasen, D. M. Tanenbaum, M. Hermenau, E. Voroshazi, M. T. Lloyd, Y. Galagan, B. Zimmernann, S. Kudret, W. Maes, L. Lutsen, D. Vanderzande, U. Wurfel, R. Andriessen, R. Rosch, H. Hoppe, G. Teran-Escobar, M. Lira-Cantu, A. Rivaton, G. Y. Uzunoglu, D. S. Germack, M. Hösel, H. F. Dam, M. Jørgensen, S. A. Gevorgyan, M. V. Madsen, E. Bundgaard, F. C. Krebs, K. Norrman, *Phys. Chem. Chem. Phys.* **2012**, *14*, 11780–11799.

[55] G. Teran-Escobar, D. M. Tanenbaum, E. Voroshazi, M. Hermenau, K. Norrman, M. T. Lloyd, Y. Galagan, B. Zimmermann, M. Hösel, H. F. Dam, M. Jørgensen, S. Gevorgyan, S. Kudret, W. Maes, L. Lutsen, D. Vanderzande, U. Wurfel, R. Andriessen, R. Rosch, H. Hoppe, A. Rivaton, G. Y. Uzunoglu, D. Germack, B. Andreasen, M. V. Madsen, E. Bundgaard, F. C. Krebs, M. Lira-Cantu, *Phys. Chem. Chem. Phys.* **2012**, *14*, 11824–11845.

[56] R. Rosch, D. M. Tanenbaum, M. Jørgensen, M. Sealand, M. Barenklau, M. Hermenau, E. Voroshazi, M. T. Lloyd, Y. Galagan, B. Zimmermann, U. Wurfel, M. Hösel, H. F. Dam, S. Gevorgyan, S. Kudret, W. Maes, L.

Lutsen, D. Vanderzande, R. Andriessen, G. Teran-Escobar, M. Lira-Cantu, A. Rivaton, G. Y. Uzunoglu, D. Germack, B. Andreasen, M. V. Madsen, K. Norrman, H. Hoppe, F. C. Krebs, *Energy Environ. Sci.* **2012**, *5*, 6521–6540.

[57] H. Neugebauer, C. J. Brabec, J. C. Hummelen, R. A. J. Janssen, N. S. Sariciftci, *Synth. Met.* **1999**, *102*, 1002–1003.

[58] M. Manceau, A. Rivaton, J. L. Gardette, S. Guillerez, N. Lemaitre, *Sol. Energy Mater. Sol. Cells* **2011**, *95*, 1315–1325.

[59] F. Padinger, T. Fromherz, P. Denk, C. J. Brabec, J. Zettner, T. Hierl, N. S. Sariciftci, *Synth. Met.* **2001**, *121*, 1605–1606.

[60] T. Jeranko, H. Tributsch, N. S. Sariciftci, J. C. Hummelen, *Sol. Energy Mater. Sol. Cells* **2004**, *83*, 247–262.

[61] S. Bertho, I. Haeldermans, A. Swinnen, W. Moons, T. Martens, L. Lutsen, D. Vanderzande, J. Manca, A. Senes, A. Bonfiglio, *Sol. Energy Mater. Sol. Cells* **2007**, *91*, 385–389.

[62] R. Scurlock, B. Wang, P. Ogilby, J. Sheats, R. Clough, *J. Am. Chem. Soc.* **1995**, *117*, 10194–10202.

[63] S. Chambon, A. Rivaton, J. L. Gardette, M. Firon, L. Lutsen, *J. Polym. Sci. Part A* **2007**, *45*, 317–331.

[64] A. Rivaton, S. Chambon, M. Manceau, J. L. Gardette, N. Lemaître, S. Guillerez, *Polym. Degrad. Stab.* **2010**, *95*, 278–284.

[65] J. A. Hauch, P. Schilinsky, S. A. Choulis, R. Childers, M. Biele, C. J. Brabec, *Sol. Energy Mater. Sol. Cells* **2008**, *92*, 727–731.

[66] M. Manceau, S. Chambon, A. Rivaton, J. L. Gardette, S. Guillerez, N. Lemaître, *Sol. Energy Mater. Sol. Cells* **2010**, *94*, 1572–1577.

[67] Y. I. Lee, J. H. Youn, M. S. Ryu, J. Kim, J. Jang, H. T. Moon, *J. Appl. Phys.* **2010**, *108*, 054506.

[68] M. S. A. Abdou, S. Holdcroft, *Can. J. Chem.* **1995**, *73*, 1893–1901.

[69] M. Manceau, A. Rivaton, J. L. Gardette, S. Guillerez, N. Lemaître, *Polym. Degrad. Stab.* **2009**, *94*, 898–907.

[70] H. Hintz, H. J. Egelhaaf, L. Leuer, J. Hauch, T. Peisert, T. Chass, *Chem. Mater.* **2011**, *23*, 145–154.

[71] A. Dupuis, P. Wong-Wah-Chung, A. Rivaton, J. L. Gardette, *Polym. Degrad. Stab.* **2012**, *97*, 366–374.

[72] E. T. Hoke, I. T. Sachs-Quintana, M. T. Lloyd, I. Kauvar, W. R. Mateker, A. M. Nardes, C. H. Peters, N. Kopidakis, M. D. McGehee, *Adv. Energy Mater.* **2012**, *2*, 1351–1357.

[73] J. Zhao, A. Swinnen, G. Van Assche, J. Manca, D. Vanderzande, B. V. Mele, *J. Phys. Chem. B* **2009**, *113*, 1587–1591.

[74] S. Chambon, A. Rivaton, J. L. Gardette, M. Firon, *Sol. Energy Mater. Sol. Cells* **2008**, *92*, 785–792.

[75] H. Hoppe, N. S. Sariciftci, *J. Mater. Chem.* **2006**, *16*, 45–61.

[76] M. O. Reese, A. M. Nardes, B. L. Rupert, R. E. Larsen, D. C. Olson, M. T. Lloyd, S. E. Shaheen, D. S. Ginley, G. Rumbles, N. Kopidakis, *Adv. Funct. Mater.* **2010**, *20*, 3476–3483.

[77] F. C. Krebs, *Sol. Energy Mater. Sol. Cells* **2006**, *90*, 3633–3643.

[78] F. Deschler, A. De Sio, E. Von Hauff, P. Kutka, T. Sauermann, H. J. Egelhaaf, J. Hauch, E. Da Como, *Adv. Funct. Mater.* **2012**, *22*, 1461–1469.

[79] J. Schafferhans, A. Baumann, A. Wagenpfahl, C. Deibel, V. Dyakonov, *Org. Electron.* **2010**, *11*, 1693–1700.

[80] Y. Lin, J. A. Lim, Q. Wei, S. C. B. Mannsfeld, A. L. Briseno, J. J. Watkins, *Chem. Mater.* **2012**, *24*, 622–632.

[81] K. Sivula, C. K. Luscombe, B. C. Thompson, J. M. J. Fréchet, *J. Am. Chem. Soc.* **2006**, *128*, 13988–13989.

[82] X. Wang, C. X. Zhao, G. Xu, Z. K. Chen, F. Zhu, *Sol. Energy Mater. Sol. Cells* **2012**, *104*, 1–6.

[83] D. E. Motaung, G. F. Malgas, C. J. Arendse, *J. Mater. Sci.* **2011**, *46*, 4942–4952.

[84] S. R. Dupont, E. Voroshazi, P. Heremans, R. H. Dauskardt, *38th IEEE Photovoltaic Specialists Conference*, Austin, TX, **2012**, Art. No 6318272, 3259–3262.

[85] I. T. Sachs-Quintana, T. Heumüller, W. R. Mateker, D. E. Orozco, R. Cheacharoen, S. Sweetnam, C. J. Brabec, M. D. McGehee, *Adv. Funct. Mater.* **2014**, *24*, 3978–3985.

[86] H. Jin, J. Olkkonen, M. Tuomikoski, P. Kopola, A. Maaninen, J. Hast, *Sol. Energy Mater. Sol. Cells* **2010**, *94*, 465–470.

[87] M. Hermenau, S. Schubert, H. Klumbies, J. Fahlteich, L. Müller-Meskamp, K. Leo, M. Riede, *Sol. Energy Mater. Sol. Cells* **2012**, *97*, 102–108.

[88] G. L. Graff, R. E. Williford, P. E. Burrows, *J. Appl. Phys.* **2004**, *96*, 1840–1849.

[89] K. Norrman, N. B. Larsen, F. C. Krebs, *Sol. Energy Mater. Sol. Cells* **2006**, *90*, 2793.

[90] S. A. Gevorgyan, F. C. Krebs, *Chem. Mater.* **2008**, *20*, 4386–4390.

[91] V. M. Drakonakis, A. Savva, M. Kokonou, S. A. Choulis, *Sol. Energy Mater. Sol. Cells* **2014**, *130*, 544–550.

[92] K. Norrman, M. V. Madsen, S. A. Gevorgyan, F. C. Krebs, *J. Am. Chem. Soc.* **2010**, *132*, 16883–16892.

[93] J. Huang, P. F. Miller, J. C. de Mello, A. J. de Mello, D. D. C. Bradley, *Synth. Met.* **2003**, *139*, 569–572.

[94] E. Vitoratos, S. Sakkopoulos, E. Dalas, N. Paliatsas, D. Karageorgopoulos, F. Petraki, S. Kennou, S. A. Choulis, *Org. Electron.* **2009**, *10*, 61–66.

[95] E. Vitoratos, S. Sakkopoulos, N. Paliatsas, K. Emmanouil, S. A. Choulis, *Open J. Org. Polym. Mater.* **2012**, *2*, 7–11.

[96] E. Voroshazi, B. Verreet, A. Buri, R. Muller, D. Di Nuzzo, P. Heremans, *Org. Electron.* **2011**, *12*, 736–744.

[97] A. Savva, M. Neophytou, C. Koutsides, K. Kalli, S. A. Choulis, *Org. Electron.* **2013**, *14*, 3123–3130.

[98] M. T. Lloyd, C. H. Peters, A. Garcia, I. V. Kauvar, J. J. Berry, M. O. Reese, M. D. McGehee, D. S. Ginley, D. C. Olson, *Sol. Energy Mater. Sol. Cells* **2011**, *95*, 1382–1388.

[99] M. Wang, F. Xie, J. Du, Q. Tang, S. Zheng, Q. Miao, J. Chen, N. Zhao, J. B. Xu, *Sol. Energy Mater. Sol. Cells* **2011**, *95*, 3303–3310.

[100] M. T. Lloyd, D. C. Olson, P. Lu, E. Fang, D. L. Moore, M. S. White, M. O. Reese, D. S. Ginley, J. W. P. Hsu, *J. Mater. Chem.* **2009**, *19*, 7638–7642.

[101] L. Zhao, T. C. W. Mak, *Organometallics* **2007**, *26*, 4439–4448.

[102] Y. Dong, Y. Geng, J. Ma, R. Huang, *Organometallics* **2006**, *25*, 447–462.

[103] A. Lachkar, A. Selmani, E. Sacher, M. Leclerc, R. Mokhliss, *Synth. Met.* **1994**, *66*, 209–215.

[104] J. Nishinaga, T. Aihara, H. Yamagata, Y. Horikoshi, *J. Cryst. Growth* **2005**, *278*, 633–637.

[105] M. O. Reese, A. J. Morfa, M. S. White, N. Kopidakis, S. E. Shaheen, G. Rumbles, D. S. Ginley, *33rd IEEE Photovoltaic Specialists Conference*, San Diego, CA, **2008**.

[106] C. W. T. Bulle-Lieuwma, W. J. H. van Gennip, J. K. J. van Duren, P. Jonkheijm, R. A. J. Janssen, J. W. Niemantsverdriet, *Appl. Surf. Sci.* **2003**, *203*, 547–550.

[107] M. P. de Jong, L. J. van Ijzendoorn, M. J. A. de Voigt, *Appl. Phys. Lett.* **2000**, *77*, 2255–2257.

[108] S. D. Yambem, K. Liao, N. J. Alley, S. A. Curran, *J. Mater. Chem.* **2012**, *22*, 6894–6898.

[109] K. A. Mazzio, M. Yuan, K. Okamoto, C. K. Luscombe, *ACS Appl. Mater. Interfaces* **2011**, *3*, 271–278.

[110] J. Chen, T. L. Chen, B. S. Kim, D. A. Poulsen, J. L. Mynar, J. M. J. Fréchet, B. Ma, *ACS Appl. Mater. Interfaces* **2010**, *2*, 2679–2686.

[111] C. E. Mauldin, C. Piliego, D. Poulsen, D. A. Unruh, C. Woo, B. Ma, J. L. Mynar, J. M. J. Fréchet, *ACS Appl. Mater. Interfaces* **2010**, *2*, 2833–2838.

[112] S. Y. Leblebici, L. Catane, D. E. Barclay, T. Olson, T. L. Chen, B. Ma, *ACS Appl. Mater. Interfaces* **2011**, *3*, 4469–4474.

[113] X. Yang, J. Loos, S. C. Veenstra, W. J. H. Verhees, M. M. Wienk, J. M. Kroon, M. A. J. Michels, R. A. J. Janssen, *Nano Lett.* **2005**, *5*, 579–583.

[114] R. Tipnis, J. Bernkopf, S. Jia, J. Krieg, S. Li, M. Storch, D. Laird, *Sol. Energy Mater. Sol. Cells* **2009**, *93*, 442–446.

[115] B. Gholamkhass, S. Holdcroft, *Chem. Mater.* **2010**, *22*, 5371–5376.

[116] Z. Li, H. C. Wong, Z. Huang, H. Zhong, C. H. Tan, W. C. Tsoi, J. S. Kim, J. R. Durrant, J. T. Cabral, *Nat. Commun.* **2013**, *4*, 2227.

[117] Z. Liang, M. O. Reese, B. A. Gregg, *ACS Appl. Mater. Interfaces* **2011**, *3*, 2042–2050.

[118] T. Tromholt, M. V. Madsen, J. E. Carlé, M. Helgesen, F. C. Krebs, *J. Mater. Chem.* **2012**, *22*, 7592–7601.

[119] M. Manceau, E. Bundgaard, J. E. Carlé, O. Hagemann, M. Helgesen, R. Søndergaard, M. Jørgensen, F. C. Krebs, *J. Mater. Chem.* **2011**, *21*, 4132–4141.

[120] M. Manceau, M. Helgesen, F. C. Krebs, *Polym. Degrad. Stab.* **2010**, *95*, 2666–2669.

[121] F. C. Krebs, H. Spanggaard, *Chem. Mater.* **2005**, *17*, 5235–5237.

[122] T. Tromholt, S. A. Gevorgyan, M. Jørgensen, F. C. Krebs, K. O. Sylvester-Hvid, *ACS Appl. Mater. Interfaces* **2009**, *1*, 2768–2777.

[123] J. E. Carlé, M. Jørgensen, M. Manceau, M. Helgesen, O. Hagemann, R. Søndergaard, F. C. Krebs, *Sol. Energy Mater. Sol. Cells* **2011**, *95*, 3222–3226.

These are not the final page numbers! ↗↗

[124] M. Helgesen, T. J. Sørensen, M. Manceau, F. C. Krebs, *Polym. Chem.* **2011**, *2*, 1355–1361.

[125] J. Kim, Y. Miyamoto, B. Ma, J. M. J. Fréchet, *Adv. Funct. Mater.* **2009**, *19*, 2273–2281.

[126] J. E. Carlé, B. Andreasen, T. Tromholt, M. V. Madsen, K. Norrman, M. Jørgensen, F. C. Krebs, *J. Mater. Chem.* **2012**, *22*, 24417–24423.

[127] C. Wen, L. Lu, X. Li, *J. Appl. Polym. Sci.* **2014**, *131*, 40975.

[128] S. Kim, D. S. Chung, H. Cha, J. W. Jang, Y. Kim, J. Kang, Y. Jeong, C. Park, S. Kwon, *Sol. Energy Mater. Sol. Cells* **2011**, *95*, 432–439.

[129] C. H. Peters, I. T. Sachs-Quitana, J. P. Kastrop, S. Beaupre, M. Leclerc, M. D. Mc Gehee, *Adv. Energy Mater.* **2011**, *1*, 491–494.

[130] B. J. Worfolk, D. A. Rider, A. L. Elias, M. Thomas, K. D. Harris, J. M. Buriak, *Adv. Funct. Mater.* **2011**, *21*, 1816–1826.

[131] B. Ecker, J. C. Nolasco, J. Pallares, L. F. Marsal, J. Posdorfer, J. Parisi, E. von Hauff, *Adv. Funct. Mater.* **2011**, *21*, 2705–2711.

[132] Y. Sun, C. J. Takacs, S. R. Cowan, J. H. Seo, X. Gong, A. Roy, A. J. Heeger, *Adv. Mater.* **2011**, *23*, 2226–2230.

[133] S. Chen, J. R. Manders, S. Tsang, F. So, *J. Mater. Chem.* **2012**, *22*, 24202–24212.

[134] C. Girotto, E. Voroshazi, D. Cheyns, P. Heremans, *ACS Appl. Mater. Interfaces* **2011**, *3*, 3244–3247.

[135] V. Shrotriya, G. Li, Y. Yao, C. W. Chu, Y. Yang, *Appl. Phys. Lett.* **2006**, *88*, 073508.

[136] J. Meyer, S. Hamwi, M. Kroger, W. Kowalsky, T. Riedl, A. Kahn, *Adv. Mater.* **2012**, *24*, 5408–5427.

[137] M. D. Irwin, D. B. Buchholz, A. W. Hains, R. P. H. Chang, T. J. Marks, *Proc. Natl. Acad. Sci. USA* **2008**, *105*, 2783–2787.

[138] S. Murase, Y. Yang, *Adv. Mater.* **2012**, *24*, 2459–2462.

[139] D. Kim, J. Subbiah, G. Sarasqueta, F. So, H. Ding, Irfan, Y. Gao, *Appl. Phys. Lett.* **2009**, *95*, 093304.

[140] H. Choi, B. Kim, M. Ko, D. Lee, H. Kim, S. Kim, K. Kim, *Org. Electron.* **2012**, *13*, 959–968.

[141] S. Han, W. S. Shin, M. Seo, D. Gupta, S. Moon, S. Yoo, *Org. Electron.* **2009**, *10*, 791–797.

[142] J. Kettle, H. Waters, M. Horie, S. Chang, *J. Phys. D* **2012**, *45*, 125102–125109.

[143] S. T. Zhang, Y. C. Zhou, J. M. Zhao, Y. Q. Zhan, Z. J. Wang, Y. Wu, X. M. Ding, X. Y. Hou, *Appl. Phys. Lett.* **2006**, *89*, 043502.

[144] C. J. Brabec, S. E. Shaheen, C. Winder, N. S. Sariciftci, *Appl. Phys. Lett.* **2002**, *80*, 1288–1290.

[145] M. Wang, Q. Tang, J. An, F. Xie, J. Chen, S. Zheng, K. Wong, Q. Miao, J. Xu, *ACS Appl. Mater. Interfaces* **2010**, *2*, 2699–2702.

[146] K. Kawano, C. Adachi, *Appl. Phys. Lett.* **2010**, *96*, 053307.

[147] M. Wang, F. Xie, W. Xie, S. Zheng, N. Ke, *Appl. Phys. Lett.* **2011**, *98*, 183304.

[148] Y. Wang, L. Yang, C. Yao, W. Qin, S. Yin, F. Zhang, *Sol. Energy Mater. Sol. Cells* **2011**, *95*, 1243–1247.

[149] L. Yang, H. Xu, H. Tian, S. Yin, F. Zhang, *Sol. Energy Mater. Sol. Cells* **2010**, *94*, 1831–1834.

[150] J. Li, S. Kim, S. Edington, J. Nedy, S. Cho, K. Lee, A. J. Heeger, M. C. Gupta, J. T. Yates, Jr., *Sol. Energy Mater. Sol. Cells* **2011**, *95*, 1123–1130.

[151] K. Lee, J. Y. Kim, S. H. Park, S. H. Kim, S. Cho, A. J. Heeger, *Adv. Mater.* **2007**, *19*, 2445–2449.

[152] M. R. Lilliedal, A. J. Medford, M. V. Madsen, K. Norrman, F. C. Krebs, *Sol. Energy Mater. Sol. Cells* **2010**, *94*, 2018–2031.

[153] S. R. Dupont, M. Oliver, F. C. Krebs, R. H. Dauskardt, *Sol. Energy Mater. Sol. Cells* **2012**, *97*, 171–175.

[154] F. C. Krebs, N. Espinosa, M. Hösel, R. Søndergaard, M. Jørgensen, *Adv. Mater.* **2014**, *26*, 29–39.

[155] E. Georgiou, A. Savva, M. Neophytou, F. Hermerschmidt, T. Demosthenous, S. A. Choulis, *Appl. Phys. Lett.* **2014**, *105*, 233901.

[156] T. R. Andersen, H. F. Dam, M. Hösel, J. E. Carlé, T. T. Larsen-Olsen, S. A. Gevorgyan, J. W. Andreasen, J. Adams, N. Li, F. Machui, G. D. Spyropoulos, T. Ameri, N. Lemaître, A. Scheel, D. Gaiser, K. Kreul, S. Berny, O. R. Lozman, S. Nordman, M. Välimäki, M. Vilkman, R. R. Søndergaard, M. Jørgensen, C. J. Brabec, F. C. Krebs, *Energy Environ. Sci.* **2014**, *7*, 2925–2933.

[157] J. S. Yu, I. Kim, J. S. Kim, J. Jo, T. T. Larsen-Olsen, R. R. Søndergaard, M. Hösel, D. Angmo, M. Jørgensen, F. C. Krebs, *Nanoscale* **2012**, *4*, 6032–6040.

[158] D. Angmo, S. A. Gevorgyan, T. T. Larsen-Olsen, R. Søndergaard, M. Hösel, M. Jørgensen, R. Gupta, G. U. Kulkarni, F. C. Krebs, *Org. Electron.* **2013**, *14*, 984–994.

[159] F. C. Krebs, J. Fyenbo, D. M. Tanenbaum, S. A. Gevorgyan, R. Andriessen, B. van Remoortere, Y. Galagand, M. Jørgensen, *Energy Environ. Sci.* **2011**, *4*, 4116–4123.

[160] D. Angmo, P. M. Sommeling, R. Gupta, M. Hösel, S. A. Gevorgyan, J. M. Kroon, G. U. Kulkarni, F. C. Krebs, *Adv. Eng. Mater.* **2014**, *16*, 976–987.

[161] P. Sommer-Larsen, M. Jørgensen, R. Søndergaard, M. Hösel, F. C. Krebs, *Energy Technol.* **2013**, *1*, 15–19.

[162] G. A. dos Reis Benatto, B. Roth, M. V. Madsen, M. Hösel, R. Søndergaard, M. Jørgensen, F. C. Krebs, *Adv. Energy Mater.* **2014**, *4*, 1400732.

[163] T. T. Larsen-Olsen, R. Søndergaard, K. Norrman, M. Jørgensen, F. C. Krebs, *Energy Environ. Sci.* **2012**, *5*, 9467–9471.

[164] J. D. Kotlarski, P. W. M. Blom, *Appl. Phys. Lett.* **2012**, *100*, 013306.

[165] F. Zhang, X. Xu, W. Tang, J. Zhang, Z. Zhuo, J. Wang, J. Wang, Z. Xu, Y. Wang, *Sol. Energy Mater. Sol. Cells* **2011**, *95*, 1785–1799.

[166] Y. Sahin, S. Alem, R. de Bettignies, J. M. Nunzi, *Thin Solid Films* **2005**, *476*, 340–343.

[167] S. K. Hau, H. Yip, N. S. Baek, J. Zou, K. O'Malley, A. K. Y. Jen, *Appl. Phys. Lett.* **2008**, *92*, 253301.

[168] Y. Lee, J. Youn, M. Ryu, J. Kim, H. Moon, J. Jang, *Org. Electron.* **2011**, *12*, 353–357.

[169] S. Cros, R. de Bettignies, S. Berson, S. Bailly, P. Maisse, N. Lemaître, S. Guillerez, *Sol. Energy Mater. Sol. Cells* **2011**, *95*, 65–69.

[170] H. H. Liao, L. M. Chen, Z. Xu, G. Li, Y. Yang, *Appl. Phys. Lett.* **2008**, *92*, 173303.

[171] K. Zilberberg, S. Trost, H. Schmidt, T. Riedl, *Adv. Energy Mater.* **2011**, *1*, 377–381.

[172] C. P. Chen, Y. D. Chen, S. C. Chuang, *Adv. Mater.* **2011**, *23*, 3859–3863.

[173] B. Zimmermann, U. Wurfel, M. Niggemann, *Sol. Energy Mater. Sol. Cells* **2009**, *93*, 491–496.

[174] M. Lin, C. Lee, S. Shiua, I. Wang, J. Sun, W. Wu, Y. Lin, J. Huang, C. Lin, *Org. Electron.* **2010**, *11*, 1828–1834.

[175] C. S. Kim, S. S. Lee, E. D. Gomez, J. B. Kim, Y. Loo, *Appl. Phys. Lett.* **2009**, *94*, 113302.

[176] H. Zhang, J. Ouyang, *Appl. Phys. Lett.* **2010**, *97*, 063509.

[177] F. C. Krebs, *Polymeric Solar Cells, Materials, Design, Manufacture*, DEStech Publications, Inc., Lancaster, PA, **2010**.

[178] M. S. Ryu, HJ. Cha, J. Jang, *Sol. Energy Mater. Sol. Cells* **2010**, *94*, 152–156.

[179] H. Sun, J. Weickert, H. C. Hesse, L. Schmidt-Mende, *Sol. Energy Mater. Sol. Cells* **2011**, *95*, 3450–3454.

[180] S. Engmann, M. Machalett, V. Turkovic, R. Rösch, E. Rädlein, G. Gobsch, H. Hoppe, *J. Appl. Phys.* **2012**, *112*, 034517.

[181] J. S. Lewis, M. S. Weaver, *Quantum Electron.* **2004**, *10*, 45–48.

[182] J. A. Hauch, P. Schilinsky, S. A. Choulis, S. Rajoelson, C. J. Brabec, *Appl. Phys. Lett.* **2008**, *93*, 103306.

[183] J. S. Lewis, *Mater. Today* **2006**, *9*, 38–45.

[184] S. Schuller, P. Schilinsky, J. Hauch, C. J. Brabec, *Appl. Phys. A* **2004**, *79*, 37–40.

[185] M. Kaltenbrunner, M. S. White, E. D. Glowacki, T. Sekitani, T. Someya, N. S. Sariciftci, S. Bauer, *Nat. Commun.* **2012**, *3*, 770.

[186] G. Dennler, C. Lungenschmied, H. Neugebauer, N. S. Sariciftci, M. Latreche, G. Czeremuszkin, M. R. Wertheimer, *Thin Solid Films* **2006**, *349*, 511–512.

[187] Y. Leterrier, *Prog. Mater. Sci.* **2003**, *48*, 1–55.

[188] A. S. da Silva Sobrinho, M. Latreche, G. Czeremuszkin, J. E. Klemberg-Sapieha, M. R. Wertheimer, *J. Vac. Sci. Technol. A* **1998**, *16*, 3190–3196.

[189] G. Dennler, C. Lungenschmied, H. Neugebauer, NS. Sariciftci, A. Labouret, *J. Mater. Res.* **2005**, *20*, 3224–3233.

[190] W. J. Potscavage, S. Yoo, B. Domercq, B. Kippelen, *Appl. Phys. Lett.* **2007**, *90*, 253511.

[191] S. Sarkar, J. H. Culp, J. T. Whyland, M. Garvan, V. Misra, *Org. Electron.* **2010**, *11*, 1896–1900.

[192] R. Toniolo, I. A. Hummelgen, *Macromol. Mater. Eng.* **2004**, *289*, 311–314.

[193] K. Agroui, G. Collins, *Sol. Energy Mater. Sol. Cells* **2003**, *80*, 33–45.

[194] K. Agroui, A. Belghachi, G. Collins, J. Farenc, *Desalination* **2007**, *209*, 1–9.

↖↖ **These are not the final page numbers!**

[195] R. R. Søndergaard, T. Makris, P. Lianos, A. Manor, E. A. Katz, W. Gong, S. M. Tuladhar, J. Nelson, R. Tuomi, P. Sommeling, S. C. Veenstra, A. Rivaton, A. Dupuis, G. T. Escobar, M. L. Cantu, S. B. Sapkota, B. Zimmermann, U. Wurfel, A. Matzarakis, F. C. Krebs, *Sol. Energy Mater. Sol. Cells* **2012**, *99*, 292–300.

[196] M. O. Reese, A. J. Morfa, M. S. White, N. Kopidakis, S. E. Shaheen, G. Rumbles, D. S. Ginley, *Sol. Energy Mater. Sol. Cells* **2008**, *92*, 746–752.

[197] C. Charton, N. Schiller, M. Fahland, A. Hollander, A. Wedel, K. Noller, *Thin Solid Films* **2006**, *502*, 99–103.

[198] A. B. Chwang, M. A. Rothman, S. Y. Mao, R. H. Hewitt, M. S. Weaver, J. A. Silvernail, K. Rajan, M. Hack, J. J. Brown, X. Chu, L. Moro, T. Krajewski, N. Rutherford, *Appl. Phys. Lett.* **2003**, *83*, 413–415.

[199] L. Moro, T. A. Krajeweski, N. M. Rutherford, O. Philips, R. J. Visser, M. E. Gross, W. D. Bennett, G. L. Graff, *Proc. SPIE-Int. Soc. Opt. Eng.* **2004**, *5214*, 83–93.

[200] S. Logothetidis, A. Laskarakis, D. Georgiou, S. Amberg-Schwab, U. Weber, K. Noller, M. Schmidt, E. Kücükpinar-Niarchos, W. Lohwasser, *Eur. Phys. J.—App. Phys.* **2010**, 51, 33203.

[201] P. Madakasira, K. Inoue, R. Ulbricht, S. B. Lee, M. Zhou, J. P. Ferraris, A. A. Zakhidov, *Synth. Met.* **2005**, *155*, 332.

[202] B. Park, Y. J. Kim, S. Graham, E. Reichmanis, *ACS Appl. Mater. Interfaces* **2011**, *3*, 3545–3551.

[203] M. S. Weaver, L. A. Michalski, K. Rajan, M. A. Rothman, J. A. Silvernail, P. E. Burrows, G. L. Graff, M. E. Gross, P. M. Martin, M. Hall, E. Mast, C. Bonham, W. Bennett, M. Zumhoff, *Appl. Phys. Lett.* **2002**, *81*, 2929–2931.

[204] J. H. Park, S. G. Oh, *Mater. Res. Bull.* **2009**, *44*, 110–118.

[205] J. Park, H. Ham, Y. Kim, J. Lee, J. Park, *Photovoltaic Specialists Conference (PVSC)*, 37th IEEE, Seattle, WA, **2011**.

[206] T. Kuwabara, T. Nakayama, K. Uozumi, T. Yamaguchi, K. Takahashi, *Sol. Energy Mater. Sol. Cells* **2008**, *92*, 1476–1482.

[207] A. J. Medford, M. R. Lilliedal, M. Jørgensen, D. Aaro, H. Pakalski, J. Fyenbo, F. C. Krebs, *Opt. Express* **2010**, *18*, 272–285.

[208] J. Adams, G. D. Spyropoulos, M. Salvador, N. Li, S. Strohm, L. Lucera, S. Langner, F. Machui, H. Zhang, T. Ameri, M. M. Voigt, F. C. Krebs, C. J. Brabec, *Energy Environ. Sci.* **2014**, *8*, 169–176.

[209] D. M. Tanenbaum, H. F. Dam, R. Rosch, M. Jørgensen, H. Hoppe, F. C. Krebs, *Sol. Energy Mater. Sol. Cells* **2012**, *97*, 157–163.

[210] S. B. Sapkota, A. Spies, B. Zimmermann, I. Dürr, U. Würfel, *Sol. Energy Mater. Sol. Cells* **2014**, *130*, 144–150.

[211] M. Hösel, R. Søndergaard, M. Jørgensen, F. C. Krebs, *Adv. Eng. Mater. Adv. Eng. Mater.* **2013**, *15*, 1068–1075.

[212] F. C. Krebs, M. Hösel, M. Corazza, B. Roth, M. V. Madsen, S. A. Gevorgyan, R. Søndergaard, D. Karg, M. Jørgensen, *Energy Technol.* **2013**, *1*, 378–381.

These are not the final page numbers! ↗↗

REVIEWS

M. Giannouli,* V. M. Drakonakis, A. Savva,
P. Eleftheriou, G. Florides, S. A. Choulis

■■ – ■■

**Methods for Improving the Lifetime
Performance of Organic Photovoltaics
with Low-Costing Encapsulation**
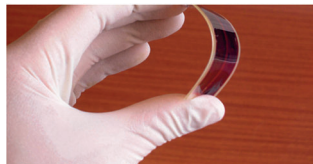
Getting to the core of it: Recent advances in improving the stability and lifetime of organic photovoltaics (OPVs) are reviewed. New materials are developed to replace those responsible for the rapid degradation of OPVs in each part of the device. Major breakthroughs leading to improved device stability include inverted device structures, the use of more photostable active-layer materials, and the introduction of interfacial buffer layers.

↖↖ **These are not the final page numbers!**